

Published in final edited form as:

Sci Transl Med. 2022 October 05; 14(665): eabh2369. doi:10.1126/scitranslmed.abh2369.

NOS1 mutations cause hypogonadotropic hypogonadism with sensory and cognitive deficits: reversal with NO therapy in infantile mice

Konstantina Chachlaki^{1,2,3,4,5,*}, Andrea Messina^{3,4,*}, Virginia Delli^{1,2,Ψ}, Valerie Leysen^{1,2,Ψ}, Csilla Murnyi⁶, Chieko Huber⁷, Gaëtan Ternier^{1,2}, Katalin Skrapits⁶, Georgios Papadakis^{3,4}, Sonal Shruti^{1,2}, Maria Kapanidou⁸, Xu Cheng^{3,4}, James Acierno^{3,4}, Jesse Rademaker^{3,4}, S Rasika^{1,2}, Richard Quinton⁹, Marek Niedziela¹⁰, Dagmar L'Allemand¹¹, Duarte Pignatelli¹², Mirjam Dirlewander¹³, Mariarosaria Lang-Muritano¹⁴, Patrick Kempf¹⁵, Sophie Catteau-Jonard^{1,2,16}, Nicolas J. Niederländer^{3,4}, Philippe Ciofi¹⁷, Manuel Tena-Sempere^{18,19,20}, John Garthwaite²³, Laurent Storme^{2,21}, Paul Avan²², Erik Hrabovszky⁶, Alan Carleton⁷, Federico Santoni^{3,4}, Paolo Giacobini^{1,2}, Nelly Pitteloud^{3,4,©,*}, Vincent Prevot^{1,2,©,*}

¹Univ. Lille, CHU Lille, Inserm, Laboratory of Development and Plasticity of the Neuroendocrine Brain, Lille Neuroscience and Cognition, UMR-S 1172, F-59000 Lille, France

²FHU 1,000 days for Health, School of Medicine, F-59000 Lille, France

³Service of Endocrinology, Diabetology, and Metabolism, Lausanne University Hospital, 1011 Lausanne, Switzerland

⁴Faculty of Biology and Medicine, University of Lausanne, Lausanne 1005, Switzerland

⁵University Research Institute of Child Health and Precision Medicine, National and Kapodistrian University of Athens, "Aghia Sophia" Children's Hospital, Athens, Greece

⁶Laboratory of Reproductive Neurobiology, Institute of Experimental Medicine, 43 Szigony St., Budapest 1083 Hungary

⁷Department of Basic Neurosciences, Faculty of Medicine, University of Geneva, 1 rue Michel-Servet, 1211 Geneva, Switzerland

© Corresponding authors: Vincent Prevot (Vincent.prevot@inserm.fr; +33 612-90-38-76) and Nelly Pitteloud (Nelly.Pitteloud@chuv.ch).

*These authors contributed equally

ΨThese authors contributed equally

Author contributions: K.C. and V.P. applied for funding, designed the preclinical study, analyzed data, prepared the figures, and wrote the manuscript along with N.P. and A.M. K.C., V.D. and V.L. designed and performed preclinical mouse studies. K.C., G.T. and P.G., studied GnRH neuronal migration in mice and human fetuses. N.P. designed the genetic approach in CHH patients and analyzed the data together with A.M., J.A., R.J., F.S., and K.C. G.P. and X.C., collected patient data. M.K. performed *in silico* analyses. K.C., A.M., N.J.N., and V.D. validated mutations *in vitro*. C.M., K.S. and E.H. designed and performed immunohistochemical analyses in the adult human hypothalamus. P.C. studied NOS1 and NK3R expression in the arcuate nucleus of intact and gonadectomized mice. S.S. designed and performed electrophysiological analyses. P.A. and V.L. assessed auditory performances in mice. C.H. and A.C. performed the attentional set-shifting task in mice. M.T.S. assessed FSH and LH levels in mice. G.T. and P.G. developed the tissue clearing approaches. S.C.J. provided human fetuses and R.Q., M.N., D.L. D.P., M.D., M.L.M., P.K. contributed patient data and material. K.C. and L.S. designed inhaled NO and sildenafil therapy in mice. K.C. and J.G. engineered the live NO/cGMP sensors. J.A. and S.R. edited the manuscript and all authors have contributed to the preparation of the manuscript.

Declaration of interests: Authors do not have any competing interests.

⁸Department of Biological and Medical Sciences, Faculty of Health and Life Sciences, Oxford Brookes University, Oxford OX3 0BP, UK

⁹Translational & Clinical Research Institute and the Royal Victoria Infirmary, University of Newcastle-upon-Tyne NE1 3BZ, UK

¹⁰Department of Paediatric Endocrinology and Rheumatology, Poznan University of Medical Sciences, Poznan, Poland

¹¹Department of Endocrinology, Children's Hospital of Eastern Switzerland, St. Gallen, Switzerland

¹²Department of Endocrinology, Hospital S João; Department of Biomedicine, Faculty of Medicine of the University of Porto; IPATIMUP Research Institute, Porto, Portugal

¹³Pediatric Endocrine and Diabetes Unit, Children's Hospital, University Hospitals and Faculty of Medicine, Geneva, CH1205, Switzerland

¹⁴Division of Pediatric Endocrinology and Diabetology and Children's Research Centre, University Children's Hospital, Zurich, Switzerland

¹⁵Department of Diabetes, Endocrinology, Clinical Nutrition & Metabolism, Inselspital, Bern University Hospital, University of Bern, Switzerland

¹⁶Department of Gynaecology and Obstetric, Jeanne de Flandres Hospital, Centre Hospitalier Universitaire de Lille, F-59000 Lille, France

¹⁷Inserm, U1215, Neurocentre Magendie, Université de Bordeaux, F-33077 Bordeaux, France

¹⁸Department of Cell Biology, Physiology and Immunology, University of Cordoba, Cordoba, Spain

¹⁹Instituto Maimonides de Investigación Biomédica de Cordoba (IMIBIC/HURS), Cordoba, Spain

²⁰CIBER Fisiopatología de la Obesidad y Nutrición, Instituto de Salud Carlos III, Cordoba, Spain

²¹Department of Neonatology, Hôpital Jeanne de Flandre, CHU of Lille, F-59000, France

²²Université de Clermont-Ferrand, Clermont-Ferrand, France

²³The Wolfson Institute for Biomedical Research, University College London, London, UK

Abstract

Background—The nitric oxide (NO) signaling pathway in hypothalamic neurons plays a key role in the regulation of the secretion of gonadotropin-releasing hormone (GnRH), crucial for reproduction. We hypothesized that a disruption of neuronal NO synthase (NOS1) activity underlies some forms of hypogonadotropic hypogonadism.

Methods—Whole exome sequencing was performed on a large cohort of probands with congenital hypogonadotropic hypogonadism to identify ultra-rare variants in *NOS1*. The activity of NOS1 mutants identified was assessed by their ability to promote nitrite and cGMP production *in vitro*. In addition, physiological and pharmacological characterization was carried out in a *Nos1*-deficient mouse model.

Findings—We identified 5 heterozygous *NOS1* loss-of-function mutations in 6 probands with congenital hypogonadotropic hypogonadism (2%), who displayed additional phenotypes including anosmia, hearing loss and intellectual disability. In addition, NOS1 was found to be transiently expressed by newly born GnRH neurons in the nose of both humans and mice, and *Nos1* deficiency in mice resulted in dose-dependent defects not only in sexual maturation but also olfaction, hearing and cognition. The pharmacological inhibition of NO production in infantile mice revealed a critical time window during which *Nos1* activity shaped minipuberty and sexual maturation. Inhaled NO treatment at minipuberty rescued both reproductive and behavioral phenotypes in *Nos1*-deficient mice.

Interpretation—The lack of timely NOS1 activity causes GnRH deficiency and lifelong sensory and intellectual comorbidities in humans and mice. NO treatment during a critical window, by reversing deficits in sexual maturation, olfaction and cognition in *Nos1*-deficient mice, thus holds therapeutic potential for humans.

Introduction

Pulsatile secretion of gonadotropin-releasing hormone (GnRH) is critical for the activation of the hypothalamic-pituitary-gonadal (HPG) axis, which controls pubertal onset and fertility. The HPG axis is transiently activated during late fetal development and again during early infancy, a phenomenon termed “minipuberty”, remains dormant during childhood, and is finally reactivated during puberty onset.

Congenital hypogonadotropic hypogonadism (CHH) is a rare genetic form of GnRH deficiency characterized by failure of puberty and infertility. CHH is associated with anosmia in approximately 50% of cases, in which case it is termed Kallmann syndrome (KS) (1). Other phenotypes such as sensorineural hearing loss (2), skeletal defects and cognitive or mental disorders (3, 4) also occur in CHH with variable frequencies. Notably, although rarely studied, the transient HPG axis activation during minipuberty is also thought to be altered in CHH (1). The consequences of altered minipuberty are largely unknown beyond defects in testicular descent and penile growth, but could impact the timing of puberty and reproductive fitness (5, 6) in the context of the early programming theory (7).

The genetics of CHH is heterogeneous. Mutations in more than 40 genes, acting either alone or in combination, have been identified in 50% of cases (8). Inactivating mutations in GnRH (*GNRH1*) (9) or GnRH receptor (*GNRHR*) (10) confirm the essential role of GnRH in reproduction. Furthermore, mutations in other CHH genes (1) have been critical to unraveling the complex biological processes affecting GnRH neuronal fate specification, migration during embryonic development and/or GnRH secretion/action in adulthood (1). Of these, inactivating mutations in genes encoding kisspeptin (*KISS1*) (11) and its receptor (*KISS1R*) (12, 13) have pinpointed the kisspeptin system as a potent upstream activator of GnRH neurons (1). Hypothalamic kisspeptin neurons are estradiol-sensitive and convey feedback from gonadal steroids to GnRH neurons, an action that requires the priming of the latter by nitric oxide (NO) release (14). Kisspeptin also directly acts on NO synthase (*Nos1*) neurons, another estrogen-responsive population regulating GnRH neurons (15, 16).

NO, which acts by stimulating the production of cyclic GMP (cGMP), is involved in a wide range of biological processes in both humans and mice, including neuronal development and plasticity (17, 18). The duration and intensity of NO signaling are modulated by phosphodiesterases (PDEs), which hydrolyze cGMP (19). In the hypothalamus, neuronal NO acts on GnRH neurons as a strong inhibitory signal that integrates both metabolic and gonadal information (19). In addition, *Nos1*-deficient mice exhibit infertility (20). We thus hypothesized that loss-of-function mutations in *NOS1* could lead to GnRH deficiency and CHH by affecting key hypothalamic neuronal circuits controlling fertility.

Results

Nos1 Distribution in the Fetal and Adult Human Hypothalamus

We examined NOS1 expression during prenatal development and in adult humans using immunohistochemistry. In the nose of human fetuses, NOS1 expression was observed in some migrating GnRH neurons but lost once they reached the forebrain region (Figure 1a).

In adult patient brains, NOS1-expressing neurons were widely distributed in the hypothalamus (Figure S1a), intermingling and interacting morphologically with GnRH neurons at various sites, including the infundibulum (Figure 1a, Figure S1b). However, GnRH neurons consistently did not co-express NOS1. Both NOS1 and GnRH neurons received input from kisspeptin neurons (Figure 1b-d). A subset ($11.4 \pm 3.0\%$) of kisspeptin neurons also expressed NOS1 (Figure 1d), a phenomenon not seen in mice, in which *Nos1* immunoreactivity is absent in neurons expressing the neurokinin B receptor NK3R (Figure S1c), used as a surrogate to identify kisspeptin neurons in the arcuate nucleus of the hypothalamus (21).

Chh Patients Harbor Heterozygous *Nos1* Mutations

NOS1 is a 29-exon gene encoding NOS1 α , a 150 kDa protein consisting of 1434 amino acids (GenBank: NM_000620.4) that functions as a homodimer (22). NOS1 α is the most commonly occurring isoform in the nervous system (19). Through exome sequencing of a large cohort of unrelated subjects with CHH ($n = 341$), we identified five ultra-rare heterozygous *NOS1* missense variants in six probands ($\sim 2\%$) (Table 1; Table S1; Figure 2). None of the probands harbored pathogenic or likely pathogenic variants in known CHH genes, according to the ACMG classification. Finally, *NOS1* missense variants were significantly enriched in our CHH cohort compared to the gnomAD control database (two-sided Fisher's exact test, $p = 2.64 \times 10^{-2}$).

The identified NOS1 mutants mapped to highly constrained sub-regions of NOS1 critical for protein function (Figure 2a,b). Three variants (p.Thr1107Met, p.Glu1124Lys and p.Ile1223Met) were located in the C-terminal reductase domain, critical for the catalytic activity of the protein. More specifically, p.Ile1223Met was located in the NAD-binding pocket and the p.Thr1107Met and p.Glu1124Lys in the FAD-binding pocket, both essential for electron transfer to the oxygenase domain of the adjacent subunit of the dimer, leading to NO formation (22). The p.Ala231Thr mutation lay within a regulatory region, the

protein inhibiting NOS1 (PIN)-binding domain, while p. Arg260Gln was located in a low-complexity region between the PIN-binding and oxygenase domains (Figure 2a).

The p.Glu1124Lys *NOS1* mutation was identified in two unrelated probands—a KS female and a normosmic CHH (nCHH) male patient. The other four mutations were found in 2 KS and 2 nCHH probands (Table 1).

Clinical Characteristics of Probands

The relevant clinical characteristics of the six probands are detailed in the supplementary materials and summarized here. Four of six probands were male. All patients presented with absent puberty, suggesting severe GnRH deficiency. Supporting this view, one male proband had a history of cryptorchidism and micropenis, consistent with altered minipuberty. Family DNA was available in four cases. All probands inherited their mutations from unaffected or partially affected parents (Figure 2b). In Family D, the female proband (II-1) harboring a p.Glu1124Lys *NOS1* mutation exhibited KS and inherited the *NOS1* mutation from her father (I-1) with constitutional delay of growth and puberty (CDGP), a transient form of GnRH deficiency (23). Hyposmia in the patient together with the presence of anosmia in her mother suggests oligogenic inheritance, although no other genetic defects in known CHH genes were identified in this pedigree (1). In addition, the male proband with KS in Family B exhibited anosmia, while the male CHH proband in Family C exhibited hyposmia. Two CHH probands (Family E, male, and Family F, female) displayed hearing loss, and one of them (Family F) also exhibited intellectual disability.

Nos1 Mutants are Loss-of-Function

Before testing the enzymatic activity of the NOS1 mutants identified above *in vitro*, we first assessed their ectopic expression after transient transfection of HEK293 cells with tagged wild-type (WT) and mutant *NOS1* cDNA. Western-blot analysis revealed that, in contrast to the WT construct, Thr1107Met and Glu1124Lys mutants were barely detectable, suggesting disrupted protein synthesis or rapid degradation (Figure 2c).

Consistent with altered expression, calcium-induced NO release using live-cell imaging was abrogated in cells transiently expressing Thr1107Met and Glu1124Lys mutants, and significantly attenuated for the 3 other reported mutants compared to cells expressing the WT plasmid ($p < 0.001$; Figure 2d-f; Figure S2a,b), suggesting decreased NOS1 activity. NOS1 requires homodimerization to enzymatically convert L-arginine and oxygen into L-citrulline and NO (24), and NOS1 mutants can impair the formation of active NOS1 dimers, resulting in reduced NO production *in vitro* (25). The decreased enzymatic activity of mutants was further confirmed using a fluorometric nitrate kit (Figure S2c). To test the possibility that NOS1 mutants impair the activity of NOS1 dimers by heterodimerizing with the NOS1 produced by the WT allele, we generated bicistronic constructs producing equimolar amounts of WT and mutated *NOS1* transcripts (Figure S2d). NOS1 activity *in vitro* was diminished to the same extent by the bicistronic construct as when cells were transfected with the mutants alone (Figure S2c), and mutant isoforms were seen to co-immunoprecipitate with WT isoforms (Figure 2g), demonstrating that the NOS1 mutants identified in our patients are dominant negative.

Nos1 Modulates GnRH Neuron Number and Migration

NO is implicated in regulating neuronal migration in the brain during mouse embryogenesis (17). We thus explored the involvement of NOS1 in GnRH neuronal migration. Similar to human fetuses (Figure 1a), in mouse embryos at embryonic day (E) 14.5, GnRH neurons co-expressed Nos1 in the nose but not the forebrain (Figure 3a). Next, we induced a transient and site-specific inhibition of NO production by infusing the NOS inhibitor L-NAME locally into the nasal region of WT mouse embryos on E12.5, when GnRH cells start to enter the rostral forebrain (Figure 3b). Blunting NO production at E12.5 resulted in a major alteration in migration (Figure 3c, d); at E14.5, the vast majority of GnRH neurons, which formed part of Nos1-immunolabeled aggregates, were arrested in the nose before entering the brain, skewing the distribution of the neurons (Figure 3c, d). However, the total number of GnRH neurons in whole heads, i.e. in both the nose and the brain, at E14.5 appeared higher in L-NAME-treated embryos at E12.5 than in littermates treated with saline in the contralateral horn of the dam's uterus (Figure 3e). To better understand the role of Nos1 in GnRH neuron migration, we evaluated the distribution and total number of GnRH neurons in the whole head, i.e., in the nose (yellow, Movie 1) and the brain (red, Movie 1) (Figure 3f) of neonatal (P0) mice lacking exon 2 of *Nos1* (*Nos1^{-/-}* mice)(26), using three-dimensional (3D) imaging and analysis of solvent-cleared tissue (iDISCO), which we have previously proven to accurately count GnRH immunolabeled neurons in the whole brain (27). Contrary to the effect of NOS inhibition by L-NAME in E14.5 embryos (Figure 3d, e), the distribution of GnRH somata at birth did not differ between *Nos1^{-/-}* mice and WT littermates (Figure 3g, Movie 2). However, as in L-NAME-injected E14.5 embryos (Figure 3e), *Nos1^{-/-}* mice showed higher total numbers of GnRH neurons at P0 (Figure 3h), suggesting that Nos1 activity may, at least in part, control the size of this neuronal population. Finally, TAG-1 immunoreactivity showed that olfactory bulb morphogenesis and olfactory and vomeronasal fiber projections to the olfactory bulb were not altered in *Nos1^{-/-}* mice (Figure 3i), suggesting preserved connectivity between the nasal epithelium and the brain in this mouse model of Nos1 deficiency.

Altered Sensory and Cognitive Performance in *Nos1*-Deficient Mice

The presence of associated phenotypes like anosmia, hearing loss and mental retardation in CHH patients harboring heterozygous *NOS1* mutations (Table 1) led us to evaluate these traits in *Nos1^{-/-}* mice, in which Nos1 activity is markedly impaired although some residual activity persists (26).

Olfaction—During the social odor discrimination test, both *Nos1^{-/-}* and *Nos1^{+/-}* mice failed to be attracted by volatile urine odors of the opposite sex (Figure 4a). During the habituation/dishabituation test, both *Nos1^{-/-}* and *Nos1^{+/-}* mice could discriminate novel non-social odors (Figure 4b). However, *Nos1^{-/-}* mice were hyper-reactive to these stimuli (Figure 4b), similar to what has been observed in premature infants during a visual habituation-dishabituation task (28, 29). The alteration of the sense of smell in *Nos1*-deficient mice thus consists of a sex-independent impairment in the encoding or processing of non-social olfactory information without gross defects in odor detection (i.e. no general anosmia).

Hearing—We studied hearing in *Nos1*-deficient mice by measuring distortion-product otoacoustic emissions. Male, but not female, *Nos1*^{-/-} mice exhibited defects in the auditory pathway at the level of the cochlear nucleus as shown by an increased latency in the auditory brainstem-evoked response (ABR) wave II (Figure 4c), and mean threshold elevations of 18.9 dB at 40 kHz (Figure 4d).

Cognition—Both *Nos1*^{-/-} and *Nos1*^{+/-} mice demonstrated defective cognitive performance compared to WT littermates in the novel object recognition test (Figure 4e). We next tested executive functions and cognitive flexibility in *Nos1*^{-/-} mice and their WT littermates using the attentional set-shifting task (30–32) (ASST) (Figure 4f), which relies on a sequence of blocks (each composed of individual trials) testing different cognitive states; each block must be completed before moving on to the next. The simple discrimination (SD) and compound discrimination blocks (CD, in which one type of sensory information serves as a distractor from another) test basic perceptual and associative abilities. The compound discrimination-reversal (CDR) block measures the ability to adjust behavior for previously learned cue-reward contingencies. The intradimensional set-shifting (IDS) block assesses attentional set formation and maintenance, while the extradimensional set-shifting (EDS) block assesses the cognitive flexibility required to disengage from previously relevant information and shift attention towards a newly relevant stimulus.

All *Nos1*^{+/+} and *Nos1*^{-/-} mice were able to complete all blocks of the ASST, with response latency being similar between genotypes (Figure 4g). Although the required number of trials to complete each block did not change between groups (Figure 4i), the pattern across blocks differed between genotypes. *Nos1*^{+/+} mice needed fewer trials to complete the IDS block than the CD block, and required more trials for the EDS block than the IDS block (Figure 4i), as previously reported for such tests (30–32), reflecting the formation of an attentional set and cognitive flexibility. *Nos1*^{+/+} mice also needed more trials to complete the CDR block than the CD block and displayed lower response accuracy (Figure 4h,i), in keeping with the increased number of trials required to suppress a previously learned cue-reward contingency due to perseverative errors (30–32). *Nos1*^{-/-} mice did not exhibit such a pattern or any sign of attentional set formation (Table S), but seemed to solve each block independently of past experience. Moreover, *Nos1*^{-/-} mice did not show any difference in the number of trials needed to complete the CDR block vs. the CD block, and committed fewer perseverative errors than *Nos1*^{+/+} mice (Figure 4h,i,j). Overall, their learning curves did not differ between the two blocks, again suggesting that *Nos1*^{-/-} mutants treated them independently (Figure 4k). In summary, *Nos1*^{-/-} mice displayed normal basic perceptual and associative abilities but impaired cognitive abilities such as reversal learning and attentional set formation.

Infantile *Nos1* Activity Shapes Minipuberty

While it is known that *Nos1*^{-/-} mice exhibit central reproductive defects and infertility (20), the underlying mechanisms are largely unknown. In a recent study, we demonstrated that *Nos1* activity increases in the preoptic region, including the organum vasculosum of the lamina terminalis (OVLT), during the infantile period (33), known to be crucial for the establishment of the GnRH neural network (19, 34, 35). Most hypothalamic *Nos1*-

expressing neurons in mice lie in the OVLT region (15), where GnRH neuronal cell bodies and dendrites also reside (15). We therefore measured immunoreactivity for Ser1412 phosphorylation-activated Nos1 (P-Nos1) (36) in the OVLT at neonatal (P7), infantile (P10 and P12) and post-weaning (P23) stages (Figure 5a, Figure S3a,b). The proportion of Nos1 neurons expressing P-Nos1 increased at P12 (Figure 5a), when high circulating FSH levels signal the occurrence of minipuberty in infantile mice (33), and persisted thereafter (Figure 5a). P-NOS1 immunoreactivity was also found in the hypothalamus of men and in women both of childbearing age and after menopause (Figure S3c). To determine whether this infantile increase in P-Nos1 expression could be linked to the FSH-induced estrogen output from the ovaries (37), we analyzed P-Nos1 expression in P23 WT mice after ovariectomy at P12, and found a striking loss of P-Nos1 immunoreactivity in the OVLT (Figure 5a, b, Figure S3a) as well as the hippocampus ($36.2 \pm 5.9\%$ vs. $10.4 \pm 2.4\%$ P-Nos1-immunoreactive Nos1 neurons, $n=3$ and 4 per group, respectively, $p=0.006$; Figure S3b). Because NO is known to restrain GnRH neuronal activity (19, 38), we next performed electrophysiological analyses in *Nos1*-deficient females at minipuberty. As expected, spontaneous firing in infantile GnRH neurons was markedly increased during the third week of life in *Gnrh::Gfp; Nos1^{-/-}* mice, compared to their *Gnrh::Gfp; Nos1^{+/+}* littermates (Figure 5c, Figure S4). This increase was associated with a precocious 4-fold increase in GnRH transcripts in *Nos1*-deficient mice compared to WT littermates at P12 rather than by P23, as shown using real-time PCR analyses of GnRH neurons after fluorescence-activated cell sorting (Figure 5d). Recent data have implicated infantile NO in *Gnrh* promoter activity during minipuberty via the transcription factor C/EBP β (33). Transcripts for the C/EBP β gene, *Cebpb*, were downregulated in GnRH neurons isolated from *Nos1*-deficient mice (Figure S5a), suggesting that, besides regulating the C/EBP β -mediated repression of the *Gnrh* promoter (33, 39), neuronal NO could also be involved in controlling the expression of this *Gnrh* promoter repressor itself. Both the increase in spontaneous firing by infantile GnRH neurons and GnRH expression (Figure 5c,d) are consistent with increased GnRH release, as shown by elevated LH and FSH levels in *Nos1*-deficient female mice at P12 (Figure 5e,5f). While post-weaning levels of FSH reached their nadir at P23 in WT mice, they remained abnormally high in *Nos1*-deficient mice and only reached control levels by P30 (Figure 5e). In contrast, LH levels at minipuberty were elevated in both *Nos1^{-/-}* and *Nos1^{+/-}* mice and reached WT levels at P23 (Figure 5f). While GnRH transcripts in the pituitary were unchanged (Figure S5b), these aberrant gonadotropin levels in *Nos1*-deficient mice were associated with blunted estradiol levels during the infantile period (Figure 5g) and increased inhibin B levels at P23 (Figure 5h), but unaltered circulating AMH (Figure 5i). Combined, these results suggest that increased Nos1 activity during minipuberty is required for the hypothalamus-driven onset of gonadal steroid negative feedback and the repression of the HPG axis at the end of minipuberty.

Puberty Is Altered in *Nos1*-Deficient Mice

The first external sign of sexual maturation, i.e. vaginal opening and first ovulation in females and balanopreputial separation in males, were altered in *Nos1^{-/-}* mice (Figure 6a-c). Vaginal opening was also delayed in *Nos1^{+/-}* females (Figure 6a). These defects were associated with abnormal estrous cyclicity and sporadic ovulatory events in young adult *Nos1^{-/-}* mice (Figure 6d).

Pharmacologically-Induced Infantile NO Deficiency Alters Sexual Maturation

To further explore the physiological role of infantile NO in the maturation of the reproductive axis, we specifically blunted NO production in WT mice between P10 and P21 by the daily intraperitoneal injection of L-NAME (50 mg/kg). This pharmacologically-induced infantile NO deficiency (Figure 6e-h) recapitulated the reproductive phenotype of genetic *Nos1*-deficient mice (Figure 6a-d), with delayed vaginal opening (Figure 6e) and pubertal onset (Figure 6f). Furthermore, infantile NO deficiency led to a deficit in adult reproductive capacity, as indicated by an increased percentage of days spent in diestrus and fewer successful ovulatory events (Figure 6g). In line with this, the typical preovulatory LH surge in adulthood (P75-90) was blunted in most infantile-NO-deficient mice (Figure 6h) when compared to vehicle-treated animals. When NO production was abolished at P7-P12, an early infantile period when FSH levels are rising (34), there was no effect on sexual maturation despite an effect on postnatal growth (Figure S6b), clearly defining the P10-P21 period as a critical window for the action of infantile NO.

Altered Sexual Maturation In *Nos1*-Deficient Mice is Rescued By no Treatment

We next investigated whether inhaled NO (iNO) during this critical period could improve the reproductive phenotype of *Nos1*-deficient mice. iNO during the P10-P23 period rescued vaginal opening (Figure 6a) and age at balanopreputial separation (Figure 6b) in both *Nos1*^{-/-} and *Nos1*^{+/-} mice and pubertal onset in females (Figure 6c), as well as estrous cyclicity in adult *Nos1*^{-/-} females (Figure 6d). Because the *Nos1*^{-/-} mouse model used in this study exhibits some residual *Nos1* activity (26), we next determined whether treatment with the selective inhibitor of cGMP-specific PDE5, Sildenafil, commonly used in human neonates as an alternative to iNO (40), could also rescue the phenotype of these mice. Daily Sildenafil injections between P10 and P23 partially normalized sexual maturation in *Nos1*^{-/-} mice (Figure 6a,c,d).

Inhaled NO Rescues Olfactory and Cognitive Impairments

Administration of iNO or Sildenafil during infancy in *Nos1*-deficient mice also restored olfactory (Figure 4a,b) and cognitive impairments in adulthood (Figure 4e), demonstrating that these neuro-developmental alterations are at least partially related *Nos1* deficiency or its consequences.

Discussion

In this study, we identified several ultra-rare heterozygous mutations of *NOS1* in 2% of our large cohort of CHH. These mutations, confirmed to be loss-of-function *in vitro*, occurred in highly constrained sub-regions of *NOS1* normally devoid of deleterious mutations in the general population (41). As observed with other CHH genes (1, 42), they were inherited from partially affected (with delayed puberty) or unaffected parents in an autosomal dominant fashion, suggesting segregation with variable expressivity and reduced penetrance.

In mice, it has been previously shown that a total loss of *Nos1* catalytic activity (i.e. deletion of the oxygenase domain) results in hypogonadism and infertility due to a central defect (20). Here, using *Nos1* knockout mice lacking exon 2 (with some residual *Nos1* activity

(26, 43)), we have demonstrated that *Nos1* deficiency impairs the onset of puberty and fertility in a dose-dependent fashion, consistent with the *Nos1* homodimerization necessary for its enzymatic action and production of NO (24, 25). This is consistent with the markedly impaired *in vitro* activity of the heterozygous *NOS1* mutants and the extreme intolerance to loss-of-function mutations of *NOS1* seen in CHH patients.

Although the hallmark of CHH is absent or partial puberty, it is currently thought that minipuberty, or the transient activation of the HPG axis during infancy, is also absent in most cases (44). Occurring during the first postnatal months in humans (45, 46) and the second week of life in rodents (34), minipuberty is characterized by a transient surge in GnRH production leading to gonadal activation. Gonadotropin profiles during minipuberty are known to be sexually dimorphic in humans (45, 46); whether similar differences occur in mice remains to be explored. In our genetically or pharmacologically *Nos1*-deprived mice, minipuberty was exaggerated and prolonged, and characterized by increased GnRH neuronal activity, higher *Gnrh* transcript expression in the hypothalamus and abnormally elevated and sustained levels of FSH. These early changes led to delayed puberty and altered fertility in adulthood, defining a critical window during which infantile NO activity shapes the postnatal maturation of the central neuroendocrine circuits driving pulsatile GnRH release. Consequently, the dynamics of GnRH release during minipuberty in humans might also shape puberty onset and adult fertility, a hypothesis that could be confirmed in CHH or CDGP patients.

NOS1 is the first gene encoding a neurotransmitter-synthesizing enzyme to be implicated in CHH. Additionally, the postnatal increase of *Nos1*-dependent NO production in the hypothalamus and hippocampus of infantile mice is also dependent on sex steroids secreted by the maturing gonads, in particular estrogen (47–49), which positively impacts the establishment of neuronal circuits in several other brain areas (50–52). Furthermore, Sildenafil, used to treat erectile dysfunction in men, also increases serum testosterone (53), and 10–20% of CHH patients exhibit a reversal of their condition after hormone therapy to normalize their sex steroid milieu (54). Among non-reproductive deficits, several probands displayed anosmia (Kallmann syndrome) or sensorineural hearing loss as well as intellectual disability, phenotypes that are also reflected in *Nos1*-deficient mice, as expected from an NO-dependent impairment of other neuronal circuits (55–57). It is thus tempting to speculate that the establishment and homeostasis of both reproductive and non-reproductive neuronal networks could contribute to the disease, and that the rise in FSH-induced estrogen production during minipuberty could act as a synchronous trigger to promote the maturation of these varied *Nos1*-dependent neuronal networks.

Anosmia in CHH is thought to result from a defect in the axonal targeting of olfactory neurons, which contribute to the migratory scaffold for GnRH neurons (1, 58, 59). However, our anatomical analyses in cleared tissues convincingly show that olfactory projections are not affected in *Nos1*^{-/-} mice. Instead, pharmacologically or genetically inhibiting *Nos1* activity during embryonic development perturbed GnRH neuronal migration from nose to brain, consistent with a temporally restricted action of NO on GnRH neuron migration, but also led to higher total number of GnRH neurons in the heads of newborn mice, suggesting that the migratory defect is either transient or compensated for by the increased

number of GnRH neurons produced. How *Nos1* activity controls the size of the GnRH neuronal population is not known. One possibility is that it does so by modulating GnRH expression through the NO-dependent transcription-factor-gene micronetwork involving C/EBP β , which represses the GnRH promoter (33). NO may also control neuronal survival by interacting with distinct signaling pathways in GnRH neurons, including with the semaphorin class 3 receptor neuropilin-1 (60), which has recently been shown to promote GnRH neuronal cell death during embryogenesis (61). In addition, the fact that not all GnRH neurons express *Nos1* suggests that there could be more than one subpopulation of these neurons with different migratory, survival and functional profiles, and the absence of *Nos1* might affect them differently.

NO is also known to modulate neural activity and synaptic transmission in the olfactory system (62, 63). NO-mediated cGMP production and the potentiation of glutamate release appear involved in the brain plasticity that underlies odor perception and memory formation related to olfaction in many different species (64–67). Importantly, NO could change olfactory capacity by altering neurogenesis and neuronal migration during development (68). The NO signaling system is ideally suited to fulfill a general presynaptic regulatory role and may effectively fine-tune network activity during embryonic and early postnatal development (69, 70), contributing to its involvement in the formation and maturation of brain circuits. Thus, the olfactory processing deficits seen in *Nos1*^{-/-} mice and at least some KS patients could be due to a modulation of synaptic plasticity and neuronal circuit synchronization in the olfactory bulb by NO/cGMP signaling emitted by GABAergic interneurons (65, 71, 72). Similarly, genes for several components of the NO/cGMP pathway are located in human deafness loci (*GUCY*, *NOS1*, *NOS2*, and *NOS3*) (73, 74), and auditory deficits, such as those found in CHH patients E and F, have been associated with alterations in the NO pathway (75, 76).

We also observed *Nos1* expression in kisspeptin neurons of the infundibulum/arcuate nucleus in humans, but not in mice. Human data were obtained in postmenopausal women. While kisspeptin expression in these patients is thought to be greatly increased due to the lack of the estrogen negative feedback, this does not detract from the finding that *NOS1* is expressed in kisspeptin neurons. However, in mice, *Nos1* expression appears to be highly positively regulated by gonadal steroids in the arcuate nucleus. Indeed, in contrast to all other hypothalamic areas analyzed, arcuate *Nos1* is absent before the minipubertal activation of the gonads and is first seen at P23 (15) and gonadectomy in adulthood dramatically dampens its expression in both sexes (Figure S1c).

The fact that intellectual disability and cognitive deficits are seen in CHH probands and *Nos1*^{-/-} mice, respectively, also reflects a broader link between NO signaling, learning ability and neurodevelopment. In the present study, the attentional set-shifting task showed that although *Nos1*^{-/-} mice displayed WT-like basic perceptual and associative abilities, their learning strategies were distinct, revealing impaired cognitive abilities due to a deficit in reversal learning and in the formation of attentional sets. The Fragile X protein, FMRP (fragile X mental retardation 1 protein), an RNA-binding protein whose loss of function is the leading monogenic cause of intellectual disability and autism, binds the *NOS1* transcript and increases its translation in the developing neocortex (71). A hypomorphic *NOS1* allele

is also associated with attention deficit hyperactivity disorder, impulsivity and aggression in humans (77), behavioral features often comorbid with Fragile X syndrome. It is also worth noting that preterm infants, who have an increased risk of developing impaired reproductive capacity (78), intellectual disability and hearing loss (79, 80), display abnormally high serum FSH levels during minipuberty (45, 46), recapitulating some phenotypic aspects of *Nos1*-deficient mice and CHH patients harboring NOS1 mutations.

The administration of exogenous NO or a PDE5 inhibitor (Sildenafil) during the critical postnatal time-window of minipuberty reversed both reproductive and non-reproductive phenotypes in our mice, confirming the crucial role played by NO. Given that iNO and sildenafil are already safely used to promote lung maturation and vascularization in premature infants, this line of treatment between the ages of 1 and 6 months may be useful to manage infants born to CHH patients and themselves carrying NOS1 mutations, to improve brain development and future quality of life. One could imagine a similar strategy to treat other disorders of pubertal development or infertility, as well as the wider spectrum of neurological deficits seen in premature infants. Indeed, the latter population constitutes a major public health issue that will only worsen with time as the age of viability of fetuses becomes progressively lower, and as viral pandemics and environmental pollutants increase the risk of preterm birth.

Our study does have some limitations. Whether CHH patients with *NOS1* mutations undergo altered minipuberty is indeed unknown, but is currently under investigation within the framework of the European miniNO consortium (<https://www.minino-project.com>). This project also aims to investigate whether iNO treatment at minipuberty could exert beneficial effects in infants at risk of developing sensory and cognitive alterations. It is also not known whether iNO or PDE5-inhibitors can, at least partly, rescue the phenotypes of adult CHH patients with NOS1 mutations. Even though our study identified a critical period for the action of *Nos1* on the establishment of the HPG axis, NO is also involved in the function of adult reproductive and non-reproductive neural circuits (19, 22), and the effects of such treatments could be investigated in *Nos1*-deficient mice in adulthood.

In summary, the broad spectrum of actions of NO in the development and homeostasis of the cardiovascular, immune and central nervous systems are well known. Our current study expands the reach of this critical molecule to include the regulation of sexual maturation and reproduction by the brain, and suggests that a safe, simple and feasible therapeutic option such as increasing NO levels during minipuberty could have far-reaching consequences for a spectrum of neurodevelopmental deficits, including in vulnerable populations such as preterm infants.

Materials and Methods

Study Design

This study designed to investigate the role of NOS1 in reproductive neuroendocrine development and adult sensory and cognitive functions was conducted in both humans and mice. Permission to use 9 gestational-week-old human Fetuses was obtained from the French Agence de Biomédecine (PFS16-002). Male and female adult human hypothalamic

tissues were obtained at autopsies from the Forensic Medicine Department of the University of Debrecen, Hungary, with the permission of the Regional Committee of Science and Research Ethics (DEOEC RKEB/IKEB: 3183-2010). The study in patients was approved by the ethics committee of the University of Lausanne (CER-VD 345/11; PB_2018-00247) and registered onto Clinicaltrials.gov with the number NCT01601171. All participants provided written informed consent prior to study participation.

All animal procedures were carried out in accordance with the guidelines for animal use specified by the European Union Council Directive of September 22, 2010 (2010/63/EU) and were approved by the Institutional Ethics Committees for the Care and Use of Experimental Animals of the Universities of Lille, Bordeaux and Geneva, and the French Department of Research (APAFIS#2617-2015110517317420v5 and #27300-2020092210299373v3) and Geneva state ethics committees. Both sexes were used in this study. Investigators were blind to the experimental group, to which age- and sex-matched littermates were assigned according to their genotype. No study size calculation was performed. No data were excluded from the study.

Patients

The CHH cohort included 341 probands (184 KS and 173 normosmic CHH [nCHH]). The diagnosis of CHH was made on the basis of: i) absent or incomplete puberty by 17 years of age; ii) low/normal gonadotropin levels in a setting of low serum testosterone/estradiol levels; and iii) otherwise normal anterior pituitary function and normal imaging of the hypothalamic-pituitary region(1). Olfaction was assessed by self-reporting and/or formal testing (81). When available, family members were included for genetic studies. This study was approved by the ethics committee of the University of Lausanne. All participants provided written informed consent prior to study participation.

Genetic Analyses

Genomic DNA was extracted from peripheral blood samples using the Puregene Blood Kit (Qiagen), following the manufacturer's protocol. Exome capture was performed using the SureSelect All Exon capture v2 or v5 (Agilent Technologies, Santa Clara, CA USA) and sequenced on the HiSeq2500 (Illumina, San Diego CA USA) at BGI (BGI, Shenzhen, PRC). Raw sequences (FASTQ files) were analyzed using an in-house pipeline that utilizes the Burrows-Wheeler Alignment algorithm (BWA)(82) for mapping the reads to the human reference sequence (GRCh37), and the Genome Analysis Toolkit (GATK)(83) for the detection of single nucleotide variants (SNVs) and insertion/deletions (Indels). The resulting variants were annotated using Annovar version 20191024(84) and dbNSFP version 4.0(85) for minor allele frequency (MAF) and pathogenicity scores.

Based on the prevalence of CHH (1), we established the MAF threshold as 0.01% and excluded all variants with a higher MAF in gnomAD. Candidate *NOS1* variants were then prioritized using the following criteria: (1) *in silico* prediction of deleteriousness (CADD (86) > 15), and (2) variant position in sub-regions highly intolerant to variation (LIMBR (41) score percentile < 5). All variants were confirmed by Sanger sequencing of both strands with duplicate PCR reactions. A gene burden analysis for the identified *NOS1* variants was

performed using a two-tailed Fisher's exact test in CHH probands vs. controls (gnomAD exome controls). Furthermore, mutations in known CHH genes (*I*) according to ACMG criteria were noted for each proband and family members harboring rare variants in *NOS1*.

Studies of Nos1 Expression

NOS1 expression was studied by immunohistochemistry in fetal heads and adult human hypothalamic tissues as described in the Supplementary Materials.

Studies of Nos1 Expression and Signaling

A human embryonic kidney cell line (HEK 293T) was transiently co-transfected with each NOS1 mutant and the FlincG3 NO-detector plasmid (pTriEx4-H6-FGAm)(87) and subjected to live imaging to assess the concentration of NO released upon the application of the calcium ionophore A23187, as described in the Supplementary Materials. NOS1 mutants expression, heterodimerization with WT NOS1 isoforms and activity were also assessed using alternative methods (see Supplementary Materials).

Assays In Mice

Neuroanatomical analyses, electrophysiological recordings and gene expression analysis in GnRH neurons, and examination of reproductive physiology and behavioral testing were carried out in male and female *Nos1*-deficient (*Nos1*^{-/-}, B6.129S4-*Nos1*tm1Plh/J) mice(26) and their *Nos1*^{+/-} and *Nos1*^{+/+} littermates, subjected or not to iNO (20ppm) or Sildenafil (15mg/kg, intraperitoneally) treatment during the infantile period (see the Supplementary Materials).

Statistical Analysis

All analyses were performed using Prism 7 (GraphPad Software, San Diego, CA) and assessed for normality (Shapiro–Wilk test) and variance, when appropriate. Sample sizes were chosen according to standard practice in the field. The investigators were blind to group allocation during the experiments. For each experiment, replicates are described in the figure legends. For animal studies, data were compared using an unpaired two-tailed Student's *t*-test or a one-way ANOVA for multiple comparisons against the control condition followed by Dunnett multiple comparison *post-hoc* test. Data not following normal distribution were analyzed using either a Mann-Whitney *U* test (comparison between two experimental groups) or Wilcoxon/Kruskal-Wallis test (comparison between three or more experimental groups) followed by a Dunn's *post hoc* analysis. The number of biologically independent experiments, sample size, *P* values, age and sex of the animals are all indicated in the main text or figure legends as well as in the statistical excel file (see data file S1) provided. All experimental data are indicated as mean ± s.e.m. The significance level was set at *P*<0.05. Symbols in figures correspond to the following significance levels: **P*<0.05, ***P*<0.001, ****P*< 0.0001. Exact *P* values and further statistical analyses are provided in Table S2 and raw data in Table S3.

Supplementary Material

Refer to Web version on PubMed Central for supplementary material.

Acknowledgments

The authors thank Professor William F. Crowley, Ravikumar Balasubramanian and Lacey Plummer (MGH Center for Genomic Medicine) for their contribution and Charlotte Laloux (behavioral exploration platform for rodents), Nathalie Jouy (cell sorting facility, BiCeL) Meryem Tardivel (imaging core facility, BiCeL) and Julien Devassine (animal house) of the PLBS UMS2014-US41 and Amandine Legrand and Gaspard Delpouve for their expert technical assistance. We thank the midwives of the Gynecology Department, Jeanne de Flandre Hospital of Lille (Centre d'Orthogenie), France, for their kind assistance and support.

Funding

This work has been supported by the European Union Horizon 2020 research and innovation program No 847941 miniNO (to K.C., L.S., F.S. N.P and V.P.), the European Research Council COST action BM1105 for the study of GnRH deficiency (to N.P., V.P., P.G., E.H., M.T.-S., P.C.) and the project No 874741 HUGODECA (to P.G.), the Fondation pour la Recherche Médicale (Equipe FRM, DEQ20130326524 to V.P and SPE201803005208 to K.C.), the Agence Nationale de la Recherche (ANR-17-CE16-0015 to V.P. and P.C.), Inserm Cross-Cutting Scientific Program (HuDeCA to P.G.), the Swiss National Foundation grants 310030_173260 (N.P.) and 310030_185292 (F.S.), Novartis Foundation (18O52 to F.S.), the Hungarian Brain Research Program (2017-1.2.1-NKP-2017-00002 to E.H.) and Hungarian Scientific Research Fund (K128317 and K138137 to E.H. and PD134837 to K.S).

Data and code availability

All the data supporting the findings of this study are available within the article and its supplementary information files.

References

- Boehm U, Bouloux PM, Dattani MT, de Roux N, Dode C, Dunkel L, Dwyer AA, Giacobini P, Hardelin JP, Juul A, Maghnie M, et al. Expert consensus document: European Consensus Statement on congenital hypogonadotropic hypogonadism--pathogenesis, diagnosis and treatment. *Nat Rev Endocrinol.* 2015; 11: 547–564. [PubMed: 26194704]
- Pingault V, Bodereau V, Baral V, Marcos S, Watanabe Y, Chaoui A, Fouveau C, Leroy C, Verier-Mine O, Francannet C, Dupin-Deguine D, et al. Loss-of-function mutations in SOX10 cause Kallmann syndrome with deafness. *Am J Hum Genet.* 2013; 92: 707–724. [PubMed: 23643381]
- Aydogan U, Aydogdu A, Akbulut H, Sonmez A, Yuksel S, Basaran Y, Uzun O, Bolu E, Saglam K. Increased frequency of anxiety, depression, quality of life and sexual life in young hypogonadotropic hypogonadal males and impacts of testosterone replacement therapy on these conditions. *Endocr J.* 2012; 59: 1099–1105. [PubMed: 22972022]
- Lasaitte L, Ceponis J, Preiksa RT, Zilaitiene B. Impaired emotional state, quality of life and cognitive functions in young hypogonadal men. *Andrologia.* 2014; 46: 1107–1112. [PubMed: 24313565]
- Kuiri-Hanninen T, Sankilampi U, Dunkel L. Activation of the hypothalamic-pituitary-gonadal axis in infancy: minipuberty. *Horm Res Paediatr.* 2014; 82: 73–80. [PubMed: 25012863]
- Lanciotti L, Cofini M, Leonardi A, Penta L, Esposito S. Up-To-Date Review About Minipuberty and Overview on Hypothalamic-Pituitary-Gonadal Axis Activation in Fetal and Neonatal Life. *Front Endocrinol (Lausanne).* 2018; 9: 410. [PubMed: 30093882]
- Barker DJ, Winter PD, Osmond C, Margetts B, Simmonds SJ. Weight in infancy and death from ischaemic heart disease. *Lancet.* 1989; 2: 577–580. [PubMed: 2570282]
- Cassatella D, Howard SR, Acierno JS, Xu C, Papadakis GE, Santoni FA, Dwyer AA, Santini S, Sykiotis GP, Chambion C, Meylan J, et al. Congenital hypogonadotropic hypogonadism and constitutional delay of growth and puberty have distinct genetic architectures. *Eur J Endocrinol.* 2018; 178: 377–388. [PubMed: 29419413]
- Bouligand J, Ghervan C, Tello JA, Brailly-Tabard S, Salenave S, Chanson P, Lombes M, Millar RP, Guiochon-Mantel A, Young J. Isolated familial hypogonadotropic hypogonadism and a GNRHI mutation. *N Engl J Med.* 2009; 360: 2742–2748. [PubMed: 19535795]

10. de Roux N, Young J, Misrahi M, Genet R, Chanson P, Schaison G, Milgrom E. A family with hypogonadotropic hypogonadism and mutations in the gonadotropin-releasing hormone receptor. *N Engl J Med.* 1997; 337: 1597–1602. [PubMed: 9371856]
11. Topaloglu AK, Tello JA, Kotan LD, Ozbek MN, Yilmaz MB, Erdogan S, Gurbuz F, Temiz F, Millar RP, Yuksel B. Inactivating KISS1 mutation and hypogonadotropic hypogonadism. *N Engl J Med.* 2012; 366: 629–635. [PubMed: 22335740]
12. Seminara SB, Messenger S, Chatzidaki EE, Thresher RR, Acierno JS Jr, Shagoury JK, Bo-Abbas Y, Kuohung W, Schwino KM, Hendrick AG, Zahn D, et al. The GPR54 gene as a regulator of puberty. *N Engl J Med.* 2003; 349: 1614–1627. [PubMed: 14573733]
13. de Roux N, Genin E, Carel JC, Matsuda F, Chaussain JL, Milgrom E. Hypogonadotropic hypogonadism due to loss of function of the KiSS1-derived peptide receptor GPR54. *Proc Natl Acad Sci U S A.* 2003; 100: 10972–10976. [PubMed: 12944565]
14. Constantin S, Reynolds D, Oh A, Pizano K, Wray S. Nitric oxide resets kisspeptin-excited GnRH neurons via PIP2 replenishment. *Proc Natl Acad Sci U S A.* 118: 2021;
15. Chachlaki K, Malone SA, Qualls-Creekmore E, Hrabovszky E, Munzberg H, Giacobini P, Ango F, Prevot V. Phenotyping of nNOS neurons in the postnatal and adult female mouse hypothalamus. *J Comp Neurol.* 2017; 525: 3177–3189. [PubMed: 28577305]
16. Hanchate NK, Parkash J, Bellefontaine N, Mazur D, Colledge WH, d'Anglemont de Tassigny X, Prevot V. Kisspeptin-GPR54 Signaling in Mouse NO-Synthesizing Neurons Participates in the Hypothalamic Control of Ovulation. *J Neurosci.* 2012; 32: 932–945. [PubMed: 22262891]
17. Mandal S, Stanco A, Buys ES, Enikolopov G, Rubenstein JL. Soluble guanylate cyclase generation of cGMP regulates migration of MGE neurons. *J Neurosci.* 2013; 33: 16897–16914. [PubMed: 24155296]
18. Charriaud-Marlangue C, Bonnin P, Pham H, Loron G, Leger PL, Gressens P, Renolleau S, Baud O. Nitric oxide signaling in the brain: a new target for inhaled nitric oxide? *Ann Neurol.* 2013; 73: 442–448. [PubMed: 23495069]
19. Chachlaki K, Garthwaite J, Prevot V. The gentle art of saying NO: how nitric oxide gets things done in the hypothalamus. *Nat Rev Endocrinol.* 2017; 13: 521–535. [PubMed: 28621341]
20. Gyurko R, Leupen S, Huang PL. Deletion of exon 6 of the neuronal nitric oxide synthase gene in mice results in hypogonadism and infertility. *Endocrinology.* 2002; 143: 2767–2774. [PubMed: 12072412]
21. Mittelman-Smith MA, Williams H, Krajewski-Hall SJ, Lai J, Ciofi P, McMullen NT, Rance NE. Arcuate kisspeptin/neurokinin B/dynorphin (KNDy) neurons mediate the estrogen suppression of gonadotropin secretion and body weight. *Endocrinology.* 2012; 153: 2800–2812. [PubMed: 22508514]
22. Chachlaki K, Prevot V. Nitric oxide signalling in the brain and its control of bodily functions. *Br J Pharmacol.* 2020; 177: 5437–5458. [PubMed: 31347144]
23. Harrington J, Palmert MR. Clinical review: Distinguishing constitutional delay of growth and puberty from isolated hypogonadotropic hypogonadism: critical appraisal of available diagnostic tests. *J Clin Endocrinol Metab.* 2012; 97: 3056–3067. [PubMed: 22723321]
24. Stuehr DJ. Structure-function aspects in the nitric oxide synthases. *Annu Rev Pharmacol Toxicol.* 1997; 37: 339–359. [PubMed: 9131257]
25. Phung YT, Black SM. Use of chimeric forms of neuronal nitric-oxide synthase as dominant negative mutants. *IUBMB Life.* 1999; 48: 333–338. [PubMed: 10690648]
26. Huang PL, Dawson TM, Bredt DS, Snyder SH, Fishman MC. Targeted disruption of the neuronal nitric oxide synthase gene. *Cell.* 1993; 75: 1273–1286. [PubMed: 7505721]
27. Casoni F, Malone SA, Belle M, Luzzati F, Collier F, Allet C, Hrabovszky E, Rasika S, Prevot V, Chedotal A, Giacobini P. Development of the neurons controlling fertility in humans: new insights from 3D imaging and transparent fetal brains. *Development.* 2016; 143: 3969–3981. [PubMed: 27803058]
28. Kavsek M, Bornstein MH. Visual habituation and dishabituation in preterm infants: a review and meta-analysis. *Res Dev Disabil.* 2010; 31: 951–975. [PubMed: 20488657]

29. Kaplan PS, Werner JS. Habituation, response to novelty, and dishabituation in human infants: tests of a dual-process theory of visual attention. *J Exp Child Psychol.* 1986; 42: 199–217. [PubMed: 3760775]
30. Tait DS, Chase EA, Brown VJ. Attentional set-shifting in rodents: a review of behavioural methods and pharmacological results. *Curr Pharm Des.* 2014; 20: 5046–5059. [PubMed: 24345263]
31. Brown VJ, Tait DS. Attentional Set-Shifting Across Species. *Curr Top Behav Neurosci.* 2016; 28: 363–395. [PubMed: 26873018]
32. Keeler JF, Robbins TW. Translating cognition from animals to humans. *Biochem Pharmacol.* 2011; 81: 1356–1366. [PubMed: 21219876]
33. Messina A, Langlet F, Chachlaki K, Roa J, Rasika S, Jouy N, Gallet S, Gaytan F, Parkash J, Tena-Sempere M, Giacobini P, et al. A microRNA switch regulates the rise in hypothalamic GnRH production before puberty. *Nat Neurosci.* 2016; 19: 835–844. [PubMed: 27135215]
34. Prevot, V. Knobil and Neill's Physiology of Reproduction. Plant, TM, Zeleznik, J, editors. Elsevier; New York: 2015. 1395–1439.
35. Pellegrino G, Martin M, Allet C, Lhomme T, Geller S, Franssen D, Mansuy V, Manfredi-Lozano M, Coutteau-Robles A, Delli V, Rasika S, et al. GnRH neurons recruit astrocytes in infancy to facilitate network integration and sexual maturation. *Nat Neurosci.* 2021; 24: 1660–1672. [PubMed: 34795451]
36. Parkash J, d'Anglemon de Tassigny X, Bellefontaine N, Campagne C, Mazure D, Buee-Scherrer V, Prevot V. Phosphorylation of N-methyl-D-aspartic acid receptor-associated neuronal nitric oxide synthase depends on estrogens and modulates hypothalamic nitric oxide production during the ovarian cycle. *Endocrinology.* 2010; 151: 2723–2735. [PubMed: 20371700]
37. Kumar TR, Wang Y, Lu N, Matzuk MM. Follicle stimulating hormone is required for ovarian follicle maturation but not male fertility. *Nat Genet.* 1997; 15: 201–204. [PubMed: 9020850]
38. Clasadonte J, Poulain P, Beauvillain JC, Prevot V. Activation of neuronal nitric oxide release inhibits spontaneous firing in adult gonadotropin-releasing hormone neurons: a possible local synchronizing signal. *Endocrinology.* 2008; 149: 587–596. [PubMed: 18006627]
39. Belsham DD, Mellon PL. Transcription factors Oct-1 and C/EBPbeta (CCAAT/enhancer-binding protein-beta) are involved in the glutamate/nitric oxide/cyclic-guanosine 5'-monophosphate-mediated repression of mediated repression of gonadotropin-releasing hormone gene expression. *Mol Endocrinol.* 2000; 14: 212–228. [PubMed: 10674395]
40. Lakshminrusimha S, Mathew B, Leach CL. Pharmacologic strategies in neonatal pulmonary hypertension other than nitric oxide. *Semin Perinatol.* 2016; 40: 160–173. [PubMed: 26778236]
41. Hayeck TJ, Stong N, Wolock CJ, Copeland B, Kamalakaran S, Goldstein DB, Allen AS. Improved Pathogenic Variant Localization via a Hierarchical Model of Sub-regional Intolerance. *Am J Hum Genet.* 2019; 104: 299–309. [PubMed: 30686509]
42. Young J, Xu C, Papadakis GE, Acierno JS, Maione L, Hietamaki J, Raivio T, Pitteloud N. Clinical Management of Congenital Hypogonadotropic Hypogonadism. *Endocr Rev.* 2019; 40: 669–710. [PubMed: 30698671]
43. Eliasson MJ, Blackshaw S, Schell MJ, Snyder SH. Neuronal nitric oxide synthase alternatively spliced forms: prominent functional localizations in the brain. *Proc Natl Acad Sci U S A.* 1997; 94: 3396–3401. [PubMed: 9096405]
44. Quinton R, Mamoojee Y, Jayasena CN, Young J, Howard S, Dunkel L, Cheetham T, Smith N, Dwyer AA. Society for Endocrinology UK guidance on the evaluation of suspected disorders of sexual development: emphasizing the opportunity to predict adolescent pubertal failure through a neonatal diagnosis of absent minipuberty. *Clin Endocrinol (Oxf).* 2017; 86: 305–306. [PubMed: 27749014]
45. Kuiri-Hanninen T, Kallio S, Seuri R, Tyrvaenen E, Liakka A, Tapanainen J, Sankilampi U, Dunkel L. Postnatal developmental changes in the pituitary-ovarian axis in preterm and term infant girls. *J Clin Endocrinol Metab.* 2011; 96: 3432–3439. [PubMed: 21900380]
46. Kuiri-Hanninen T, Seuri R, Tyrvaenen E, Turpeinen U, Hamalainen E, Stenman UH, Dunkel L, Sankilampi U. Increased activity of the hypothalamic-pituitary-testicular axis in infancy results in increased androgen action in premature boys. *J Clin Endocrinol Metab.* 2011; 96: 98–105. [PubMed: 20881260]

47. Garcia-Duran M, de Frutos T, Diaz-Recasens J, Garcia-Galvez G, Jimenez A, Monton M, Farre J, Sanchez de Miguel L, Gonzalez-Fernandez F, Arriero MD, Rico L, et al. Estrogen stimulates neuronal nitric oxide synthase protein expression in human neutrophils. *Circ Res.* 1999; 85: 1020–1026. [PubMed: 10571532]
48. d'Anglemont de Tassigny X, Campagne C, Steculorum S, Prevot V. Estradiol induces physical association of neuronal nitric oxide synthase with NMDA receptor and promotes nitric oxide formation via estrogen receptor activation in primary neuronal cultures. *J Neurochem.* 2009; 109: 214–224.
49. d'Anglemont de Tassigny X, Campagne C, Dehouck B, Leroy D, Holstein GR, Beauvillain JC, Buee-Scherrer V, Prevot V. Coupling of neuronal nitric oxide synthase to NMDA receptors via postsynaptic density-95 depends on estrogen and contributes to the central control of adult female reproduction. *J Neurosci.* 2007; 27: 6103–6114. [PubMed: 17553983]
50. McCarthy MM. Estradiol and the developing brain. *Physiol Rev.* 2008; 88: 91–124. [PubMed: 18195084]
51. McEwen B. Estrogen actions throughout the brain. *Recent Prog Horm Res.* 2002; 57: 357–384. [PubMed: 12017552]
52. Denley MCS, Gatford NJF, Sellers KJ, Srivastava DP. Estradiol and the Development of the Cerebral Cortex: An Unexpected Role? *Front Neurosci.* 2018; 12: 245. [PubMed: 29887794]
53. Carosa E, Martini P, Brandetti F, Di Stasi SM, Lombardo F, Lenzi A, Jannini EA. Type V phosphodiesterase inhibitor treatments for erectile dysfunction increase testosterone levels. *Clin Endocrinol (Oxf).* 2004; 61: 382–386. [PubMed: 15355456]
54. Raivio T, Falardeau J, Dwyer A, Quinton R, Hayes FJ, Hughes VA, Cole LW, Pearce SH, Lee H, Boepple P, Crowley WF Jr, et al. Reversal of idiopathic hypogonadotropic hypogonadism. *N Engl J Med.* 2007; 357: 863–873. [PubMed: 17761590]
55. Steinert JR, Robinson SW, Tong H, Haustein MD, Kopp-Scheinflug C, Forsythe ID. Nitric oxide is an activity-dependent regulator of target neuron intrinsic excitability. *Neuron.* 2011; 71: 291–305. [PubMed: 21791288]
56. Weitzdoerfer R, Hoeger H, Engidawork E, Engelmann M, Singewald N, Lubec G, Lubec B. Neuronal nitric oxide synthase knock-out mice show impaired cognitive performance. *Nitric Oxide.* 2004; 10: 130–140. [PubMed: 15158692]
57. Gao Y, Heldt SA. Lack of neuronal nitric oxide synthase results in attention deficit hyperactivity disorder-like behaviors in mice. *Behav Neurosci.* 2015; 129: 50–61. [PubMed: 25621792]
58. Teixeira L, Guimiot F, Dode C, Fallet-Bianco C, Millar RP, Delezoide AL, Hardelin JP. Defective migration of neuroendocrine GnRH cells in human arrhinencephalic conditions. *J Clin Invest.* 2010; 120: 3668–3672. [PubMed: 20940512]
59. Hanchate NK, Giacobini P, Lhuillier P, Parkash J, Espy C, Fouveaut C, Leroy C, Baron S, Campagne C, Vanacker C, Collier F, et al. SEMA3A, a Gene Involved in Axonal Pathfinding, Is Mutated in Patients with Kallmann Syndrome. *PLoS Genet.* 2012; 8 e1002896 [PubMed: 22927827]
60. Song H, Ming G, He Z, Lehmann M, McKerracher L, Tessier-Lavigne M, Poo M. Conversion of neuronal growth cone responses from repulsion to attraction by cyclic nucleotides. *Science.* 1998; 281: 1515–1518. [PubMed: 9727979]
61. Vanacker C, Trova S, Shruti S, Casoni F, Messina A, Croizier S, Malone S, Ternier G, Hanchate NK, Rasika S, Bouret SG, et al. Neuropilin-1 expression in GnRH neurons regulates prepubertal weight gain and sexual attraction. *EMBO J.* 2020; 39 e104633 [PubMed: 32761635]
62. Pietrobon M, Zamparo I, Maritan M, Franchi SA, Pozzan T, Lodovichi C. Interplay among cGMP, cAMP, and Ca²⁺ in living olfactory sensory neurons in vitro and in vivo. *J Neurosci.* 2011; 31: 8395–8405. [PubMed: 21653844]
63. Watanabe S, Takanashi F, Ishida K, Kobayashi S, Kitamura Y, Hamasaki Y, Saito M. Nitric Oxide-Mediated Modulation of Central Network Dynamics during Olfactory Perception. *PLoS One.* 2015; 10 e0136846 [PubMed: 26360020]
64. Fujie S, Aonuma H, Ito I, Gelperin A, Ito E. The nitric oxide/cyclic GMP pathway in the olfactory processing system of the terrestrial slug *Limax marginatus*. *Zool Sci.* 2002; 19: 15–26. [PubMed: 12025400]

65. Kendrick KM, Guevara-Guzman R, Zorrilla J, Hinton MR, Broad KD, Mimmack M, Ohkura S. Formation of olfactory memories mediated by nitric oxide. *Nature*. 1997; 388: 670–674. [PubMed: 9262400]
66. Wilson CH, Christensen TA, Nighorn AJ. Inhibition of nitric oxide and soluble guanylyl cyclase signaling affects olfactory neuron activity in the moth, *Manduca sexta*. *J Comp Physiol A Neuroethol Sens Neural Behav Physiol*. 2007; 193: 715–728. [PubMed: 17551736]
67. Hopkins DA, Steinbusch HW, Markerink-van Ittersum M, De Vente J. Nitric oxide synthase, cGMP, and NO-mediated cGMP production in the olfactory bulb of the rat. *J Comp Neurol*. 1996; 375: 641–658. [PubMed: 8930790]
68. Sulz L, Astorga G, Bellette B, Iturriaga R, Mackay-Sim A, Bacigalupo J. Nitric oxide regulates neurogenesis in adult olfactory epithelium in vitro. *Nitric Oxide*. 2009; 20: 238–252. [PubMed: 19371594]
69. Cserep C, Szonyi A, Veres JM, Nemeth B, Szabadits E, de Vente J, Hajos N, Freund TF, Nyiri G. Nitric oxide signaling modulates synaptic transmission during early postnatal development. *Cereb Cortex*. 2011; 21: 2065–2074. [PubMed: 21282319]
70. Qu GJ, Ma J, Yu YC, Fu Y. Postnatal development of GABAergic interneurons in the neocortical subplate of mice. *Neuroscience*. 2016; 322: 78–93. [PubMed: 26892297]
71. Kwan KY, Lam MM, Johnson MB, Dube U, Shim S, Rasin MR, Sousa AM, Fertuzinhos S, Chen JG, Arellano JI, Chan DW, et al. Species-dependent posttranscriptional regulation of NOS1 by FMRP in the developing cerebral cortex. *Cell*. 2012; 149: 899–911. [PubMed: 22579290]
72. Roskams AJ, Bredt DS, Dawson TM, Ronnett GV. Nitric oxide mediates the formation of synaptic connections in developing and regenerating olfactory receptor neurons. *Neuron*. 1994; 13: 289–299. [PubMed: 7520251]
73. Bowl MR, Dawson SJ. Age-Related Hearing Loss. *Cold Spring Harb Perspect Med*. 2018.
74. Shen J, Scheffer DI, Kwan KY, Corey DP. SHIELD: an integrative gene expression database for inner ear research. *Database (Oxford)*. 2015; 2015 bav071 [PubMed: 26209310]
75. Mohrle D, Reimann K, Wolter S, Wolters M, Varakina K, Mergia E, Eichert N, Geisler HS, Sandner P, Ruth P, Friebe A, et al. NO-Sensitive Guanylate Cyclase Isoforms NO-GC1 and NO-GC2 Contribute to Noise-Induced Inner Hair Cell Synaptopathy. *Mol Pharmacol*. 2017; 92: 375–388. [PubMed: 28874607]
76. Olthof BMJ, Gartside SE, Rees A. Puncta of Neuronal Nitric Oxide Synthase (nNOS) Mediate NMDA Receptor Signaling in the Auditory Midbrain. *J Neurosci*. 2019; 39: 876–887. [PubMed: 30530507]
77. Reif A, Jacob CP, Rujescu D, Herterich S, Lang S, Gutknecht L, Baehne CG, Strobel A, Freitag CM, Giegling I, Romanos M, et al. Influence of functional variant of neuronal nitric oxide synthase on impulsive behaviors in humans. *Arch Gen Psychiatry*. 2009; 66: 41–50. [PubMed: 19124687]
78. Swamy GK, Ostbye T, Skjaerven R. Association of preterm birth with long-term survival, reproduction, and next-generation preterm birth. *JAMA*. 2008; 299: 1429–1436. [PubMed: 18364485]
79. D’Onofrio BM, Class QA, Rickert ME, Larsson H, Langstrom N, Lichtenstein P. Preterm birth and mortality and morbidity: a population-based quasi-experimental study. *JAMA Psychiatry*. 2013; 70: 1231–1240. [PubMed: 24068297]
80. Moster D, Lie RT, Markestad T. Long-term medical and social consequences of preterm birth. *N Engl J Med*. 2008; 359: 262–273. [PubMed: 18635431]
81. Lewkowitz-Shpuntoff HM, Hughes VA, Plummer L, Au MG, Doty RL, Seminara SB, Chan YM, Pitteloud N, Crowley WF Jr, Balasubramanian R. Olfactory phenotypic spectrum in idiopathic hypogonadotropic hypogonadism: pathophysiological and genetic implications. *The Journal of clinical endocrinology and metabolism*. 2012; 97: E136–144. [PubMed: 22072740]
82. Li H, Durbin R. Fast and accurate short read alignment with Burrows-Wheeler transform. *Bioinformatics*. 2009; 25: 1754–1760. [PubMed: 19451168]
83. DePristo MA, Banks E, Poplin R, Garimella KV, Maguire JR, Hartl C, Philippakis AA, del Angel G, Rivas MA, Hanna M, McKenna A, et al. A framework for variation discovery and genotyping

- using next-generation DNA sequencing data. *Nature genetics*. 2011; 43: 491–498. [PubMed: 21478889]
84. Wang K, Li M, Hakonarson H. ANNOVAR: functional annotation of genetic variants from high-throughput sequencing data. *Nucleic Acids Res*. 2010; 38 e164 [PubMed: 20601685]
 85. Liu X, Jian X, Boerwinkle E. dbNSFP v2.0: a database of human non-synonymous SNVs and their functional predictions and annotations. *Human mutation*. 2013; 34: E2393–2402. [PubMed: 23843252]
 86. Kircher M, Witten DM, Jain P, O’Roak BJ, Cooper GM, Shendure J. A general framework for estimating the relative pathogenicity of human genetic variants. *Nat Genet*. 2014; 46: 310–315. [PubMed: 24487276]
 87. Bhargava Y, Hampden-Smith K, Chachlaki K, Wood KC, Vernon J, Allerston CK, Batchelor AM, Garthwaite J. Improved genetically-encoded, FlincG-type fluorescent biosensors for neural cGMP imaging. *Front Mol Neurosci*. 2013; 6: 26. [PubMed: 24068983]
 88. Amato LGL, Montenegro LR, Lerario AM, Jorge AAL, Guerra G Junior, Schnoll C, Renck AC, Trarbach EB, Costa EMF, Mendonca BB, Latronico AC, et al. New genetic findings in a large cohort of congenital hypogonadotropic hypogonadism. *Eur J Endocrinol*. 2019; 181: 103–119. [PubMed: 31200363]
 89. Messina A, Pulli K, Santini S, Acierno J, Kansakoski J, Cassatella D, Xu C, Casoni F, Malone SA, Ternier G, Conte D, et al. Neuron-Derived Neurotrophic Factor Is Mutated in Congenital Hypogonadotropic Hypogonadism. *Am J Hum Genet*. 2020; 106: 58–70. [PubMed: 31883645]
 90. Richards S, Aziz N, Bale S, Bick D, Das S, Gastier-Foster J, Grody WW, Hegde M, Lyon E, Spector E, Voelkerding K, et al. Standards and guidelines for the interpretation of sequence variants: a joint consensus recommendation of the American College of Medical Genetics and Genomics and the Association for Molecular Pathology. *Genet Med*. 2015; 17: 405–424. [PubMed: 25741868]
 91. Tang H, Thomas PD. PANTHER-PSEP: predicting disease-causing genetic variants using position-specific evolutionary preservation. *Bioinformatics*. 2016; 32: 2230–2232. [PubMed: 27193693]
 92. Ashkenazy H, Abadi S, Martz E, Chay O, Mayrose I, Pupko T, Ben-Tal N. ConSurf 2016: an improved methodology to estimate and visualize evolutionary conservation in macromolecules. *Nucleic Acids Res*. 2016; 44: W344–350. [PubMed: 27166375]
 93. Goedhart J, van Weeren L, Adjobo-Hermans MJ, Elzenaar I, Hink MA, Gadella TW Jr. Quantitative co-expression of proteins at the single cell level--application to a multimeric FRET sensor. *PLoS One*. 2011; 6 e27321 [PubMed: 22114669]
 94. Garthwaite J, Southam E, Boulton CL, Nielsen EB, Schmidt K, Mayer B. Potent and selective inhibition of nitric oxide-sensitive guanylyl cyclase by 1H-[1,2,4]oxadiazolo[4,3-a]quinoxalin-1-one. *Mol Pharmacol*. 1995; 48: 184–188. [PubMed: 7544433]
 95. Bellefontaine N, Chachlaki K, Parkash J, Vanacker C, Colledge W, d’Anglemon de Tassigny X, Garthwaite J, Bouret SG, Prevot V. Leptin-independent neuronal NO signaling in the preoptic hypothalamus facilitates reproduction. *J Clin Invest*. 2014; 124: 2550–2559. [PubMed: 24812663]
 96. Batchelor AM, Bartus K, Reynell C, Constantinou S, Halvey EJ, Held KF, Dostmann WR, Vernon J, Garthwaite J. Exquisite sensitivity to subsecond, picomolar nitric oxide transients conferred on cells by guanylyl cyclase-coupled receptors. *Proc Natl Acad Sci U S A*. 2010; 107: 22060–22065. [PubMed: 21135206]
 97. Spergel DJ, Kruth U, Hanley DF, Sprengel R, Seeburg PH. GABA- and glutamate-activated channels in green fluorescent protein-tagged gonadotropin-releasing hormone neurons in transgenic mice. *J Neurosci*. 1999; 19: 2037–2050. [PubMed: 10066257]
 98. Steyn FJ, Wan Y, Clarkson J, Veldhuis JD, Herbison AE, Chen C. Development of a methodology for and assessment of pulsatile luteinizing hormone secretion in juvenile and adult male mice. *Endocrinology*. 2013; 154: 4939–4945. [PubMed: 24092638]
 99. Fonseca H, Powers SK, Goncalves D, Santos A, Mota MP, Duarte JA. Physical inactivity is a major contributor to ovariectomy-induced sarcopenia. *Int J Sports Med*. 2012; 33: 268–278. [PubMed: 22261826]

100. Devillers MM, Petit F, Cluzet V, Francois CM, Giton F, Garrel G, Cohen-Tannoudji J, Guigon CJ. FSH inhibits AMH to support ovarian estradiol synthesis in infantile mice. *J Endocrinol.* 2019; 240: 215–228. [PubMed: 30403655]
101. Pansiot J, Loron G, Olivier P, Fontaine R, Charriaut-Marlangue C, Mercier JC, Gressens P, Baud O. Neuroprotective effect of inhaled nitric oxide on excitotoxic-induced brain damage in neonatal rat. *PLoS One.* 2010; 5 e10916 [PubMed: 20532231]
102. Hua-Huy T, Duong-Quy S, Pham H, Pansiot J, Mercier JC, Baud O, Dinh-Xuan AT. Inhaled nitric oxide decreases pulmonary endothelial nitric oxide synthase expression and activity in normal newborn rat lungs. *ERJ Open Res.* 2016; 2
103. Ambalavanan N, Aschner JL. Management of hypoxemic respiratory failure and pulmonary hypertension in preterm infants. *J Perinatol.* 2016; 36 (Suppl 2) S20–27. [PubMed: 27225961]
104. Fodoulian L, Gschwend O, Huber C, Mutel S, Salazar RF, Leone R, Renfer J-R, Ekundayo K, Rodriguez I, Carleton A. The claustrum-medial prefrontal cortex network controls attentional set-shifting. *bioRxiv.* 2020.
105. Skrapits K, Borsay BA, Herczeg L, Ciofi P, Bloom SR, Ghatei MA, Dhillon WS, Liposits Z, Hrabovszky E. Colocalization of cocaine- and amphetamine-regulated transcript with kisspeptin and neurokinin B in the human infundibular region. *PLoS One.* 2014; 9 e103977 [PubMed: 25084101]
106. Hrabovszky E, Molnar CS, Sipos MT, Vida B, Ciofi P, Borsay BA, Sarkadi L, Herczeg L, Bloom SR, Ghatei MA, Dhillon WS, et al. Sexual dimorphism of kisspeptin and neurokinin B immunoreactive neurons in the infundibular nucleus of aged men and women. *Front Endocrinol (Lausanne).* 2011; 2: 80. [PubMed: 22654828]
107. Borsay BA, Skrapits K, Herczeg L, Ciofi P, Bloom SR, Ghatei MA, Dhillon WS, Liposits Z, Hrabovszky E. Hypophysiotropic gonadotropin-releasing hormone projections are exposed to dense plexuses of kisspeptin, neurokinin B and substance p immunoreactive fibers in the human: a study on tissues from postmenopausal women. *Neuroendocrinology.* 2014; 100: 141–152. [PubMed: 25247878]
108. Swanson, LW. *Structure of the rat brain.* Elsevier Science Publishers; Amsterdam: 2004.

One-sentence summary

Altered NOS1 activity causes congenital GnRH deficiency with sensory and cognitive comorbidities, rescued experimentally by NO therapy at minipuberty.

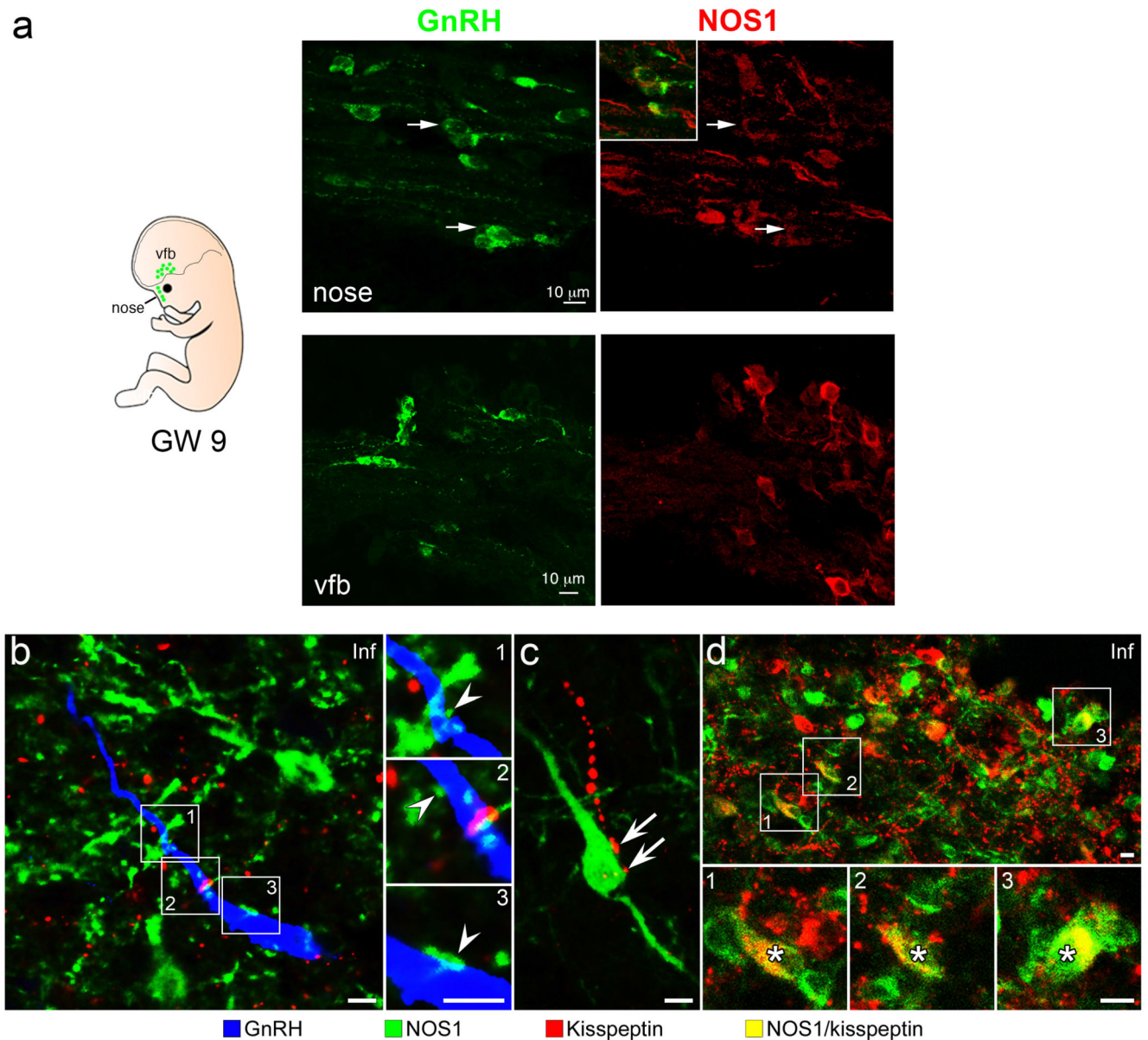


Figure 1. NOS1 expression in the GnRH neuronal system in humans

(a) 9-week old human fetus immunolabeling showing migrating GnRH neurons (green) coexpressing NOS1 protein (red) in the nose (arrows upper panels), but not in the ventral forebrain (vfb; lower panels).

(b) NOS1 (green), GnRH (blue) and Kisspeptin (red) triple-immunofluorescence in the infundibulum (Inf) of adult human hypothalamus. White arrowheads: contacts between NOS1-immunoreactive processes and GnRH neurons.

(c) Kisspeptin fibers (red) innervating (white arrows) NOS1 cells.

(d) A subpopulation of the kisspeptin neurons (asterisks) co-expressing NOS1 in the infundibulum.

Scale bars: 15 μm .

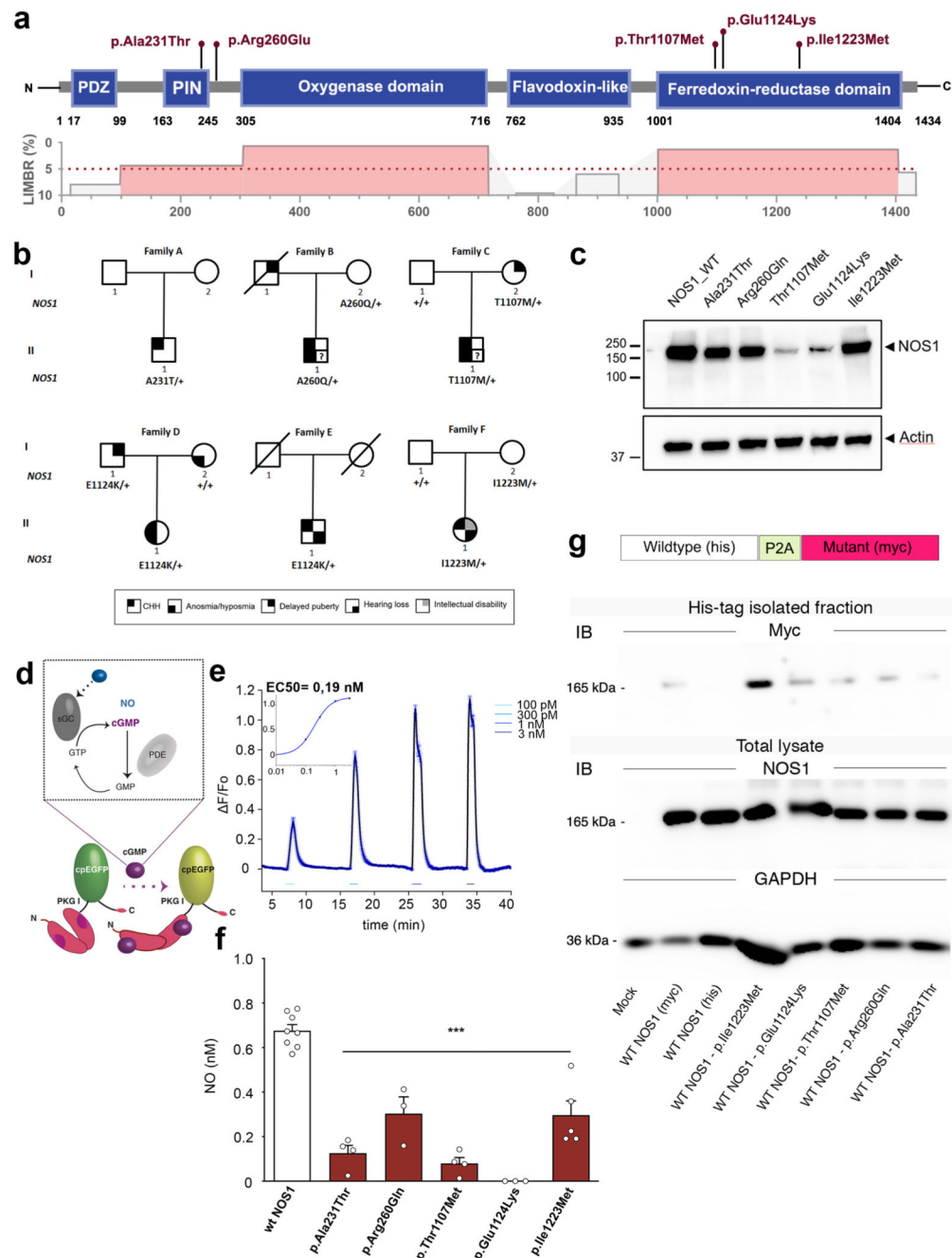


Figure 2. Identification and characterization of *NOS1* mutations in CHH probands
 (a) Lollipop plot illustrating the distribution of identified mutations in functional domains (blue boxes) of the human *NOS1* protein (upper panel) and in highly constrained sub-regions (LIMBR score < 5%; lower panel in red).
 (b) Pedigrees of CHH probands harboring *NOS1* mutations. Phenotypes are indicated by symbols as shown in the legend (bottom).
 (c) Representative western blot showing ectopic expression of *NOS1* protein (Anti-Myc tag) in HEK293 cells 48h after transfection with WT or mutant *NOS1* constructs.

(d) Mode of action of NO on the fluorometric probe (FlnG3) used to quantify NO production from NOS1 isoforms using live-cell imaging in transfected HEKGC/PDE5 cells (i.e. NO detector cells) and (e) calibrating the dose-response curve. sGC, soluble guanylate cyclase; PDE, phosphodiesterase; EGFP, enhanced green fluorescent protein; F, fluorescence.

(f) NO concentration upon endogenous stimulation of the NO signaling pathway in NO-detector cells expressing the WT or mutated NOS1 protein (one-way ANOVA with Dunnett's post-hoc test; n=8,4,3,4,3,5). ***P<0.001. Values indicate means \pm SEM. N>3 independent experiments using technical replicates.

(g) Representative Western blots showing co-immunoprecipitation of Myc-tagged NOS1 mutants with His-tagged WT NOS1.

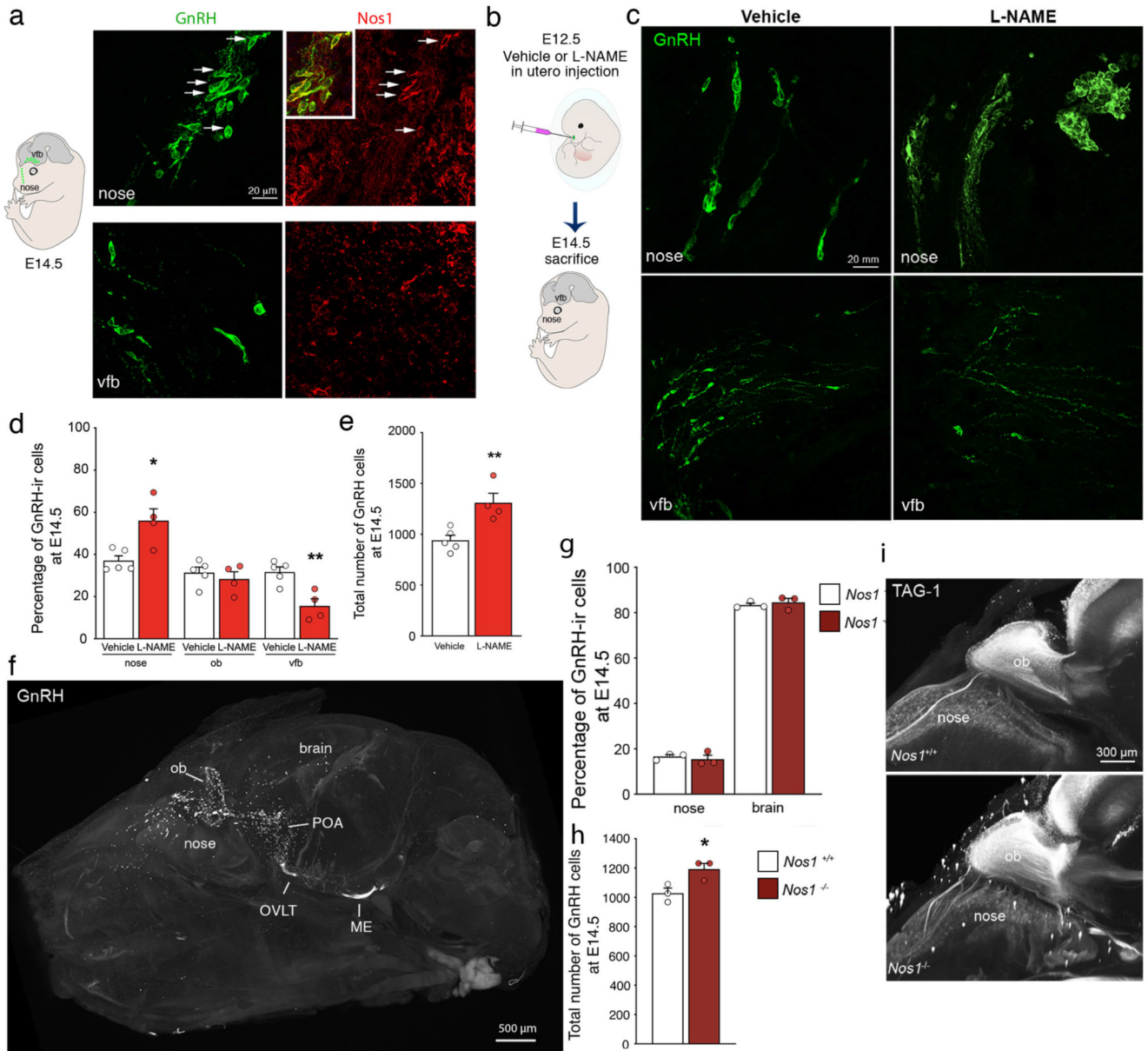


Figure 3. A role for Nos1 in GnRH neuron migration and number

(a) Immunolabeling of a mouse embryo on embryonic day (E) 14.5 showing migrating GnRH neurons (green) and Nos1 protein expression (red) in the nose (upper panels) and the ventral forebrain (vfb) (lower panels).

(b) Schematic showing *in utero* injections of L-NAME into the nose of mouse embryos at E12.

(c) Immunolabeling of a mouse embryo on E14.5 injected with vehicle (left panels) or L-NAME (right panels) showing migrating GnRH neurons (green) in the nose (upper panels) and the vfb (lower panels).

(d) Distribution and (e) total number of GnRH neurons at E14.5 in vehicle (white; n=5)- and L-NAME-treated (red; n=4) embryos in the nose, olfactory bulb (ob) and vfb.

(f) Transparentized whole head and immunofluorescence for GnRH (white) in a *Nos1^{-/-}* mouse at P0. ME, median eminence; ob, olfactory bulb; OVLT, organum vasculosum laminae terminalis; POA, preoptic region.

(g) Distribution (Kruskal-Wallis followed by Dunn's multiple comparisons), and (h) total number of the GnRH neurons in newborn *Nos1^{+/+}* (black; n=3)- and *Nos1^{-/-}* (brown; n=3) mice.

(i) Representative 3D images of TAG-1 immunoreactive olfactory fibers projecting into the brain in *Nos1^{+/+}* and *Nos1^{-/-}* littermates at P0.

Values indicate means \pm SEM. N 3 independent litters. Unpaired t-test, *P<0.05, **P<0.01.

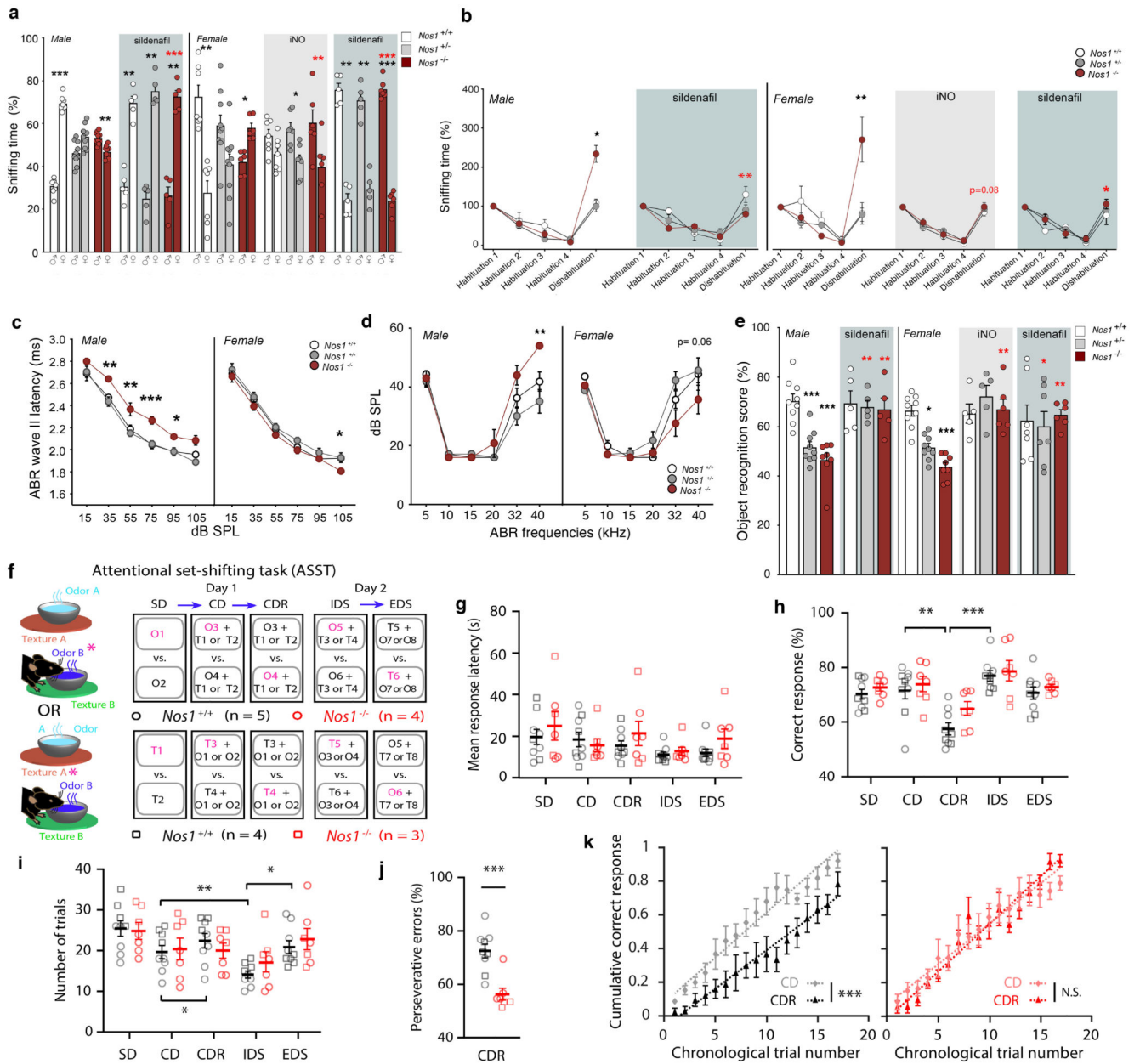


Figure 4. Behavioral tests in *Nos1*-deficient mice: olfaction, cognition and hearing.

(a) Social olfactory preference test in male and female *Nos1*^{+/+}, *Nos1*^{+/-} and *Nos1*^{-/-} mice treated or not with iNO (grey-shaded area) or Sildenafil (blue-shaded area) during the infantile period from P10 to P23. Black asterisks indicate the preference of each group for male versus female odor (paired t-test; males: untreated, n= 8,10,10; Sildenafil-treated, n=5,5,5; females: untreated n=7,10,6; Sildenafil-treated, n=5,5,6; iNO-treated, n=7,7,6). Red asterisks: comparison between mice of the same sex and genotype but subjected to different treatments [*Nos1*^{-/-} Females: Kruskal-Wallis followed by Dunn’s multiple comparisons test; *Nos1*^{-/-} males: Mann-Whitney U test].

(b) Non-social olfactory preference test in male and female *Nos1^{+/+}*, *Nos1^{+/-}* and *Nos1^{-/-}* mice treated or not with iNO (grey-shaded area), or Sildenafil (blue-shaded area) during the infantile period from P10 to P23. Values for *Nos1^{+/+}* mice during the dishabituation stage are compared to those of *Nos1^{+/-}* and *Nos1^{-/-}* mice for each treatment group [Kruskal-Wallis followed by Dunn's multiple comparisons test; males: untreated, n=6,5,5; Sildenafil-treated, n=5,5,5; females: untreated, n=7,8,7; Sildenafil-treated, n=5,5,5; iNO-treated, n=6,5,6]

(c, d) Hearing assessed by measuring (c) latencies at the level of the cochlear nucleus (distortion-product otoacoustic emissions were identical in all mice), and (d) auditory brainstem-evoked response (ABR) thresholds in *Nos1^{+/+}*, *Nos1^{+/-}* and *Nos1^{-/-}* male (n=8,8,6) and female mice (n=9,9,9). *Nos1^{+/+}* values are compared to those of *Nos1^{+/-}* and *Nos1^{-/-}* mice for each group of measurements (two-way ANOVA with Dunnett's post-hoc test).

(e) Recognition memory test in *Nos1^{+/+}*, *Nos1^{+/-}* and *Nos1^{-/-}* male and female mice treated or not (untreated males, n=9,9,8 and females, n=9,9,8) with iNO (grey-shaded area; females, n=6,5,6) or Sildenafil (blue-shaded area; males, n=5,5,5; females, n=5,5,6) during the infantile period. *Nos1^{+/+}* values are compared to those of *Nos1^{+/-}* and *Nos1^{-/-}* mice for each group of measurements (Kruskal-Wallis test with Dunn's post-hoc test). Red asterisks: comparison between mice of the same genotype but subjected to different treatments (Mann-Whitney test for males and Kruskal-Wallis test with Dunn's post-hoc test for females).

(f-k) Attentional-set formation and reversal learning in *Nos1^{+/+}* (n=9) and *Nos1^{-/-}* male mice (n=7). (f) Schematics of the attentional set-shifting task (ASST). Half the mice started the task with olfactory cues being informative (top, purple letters, circles) whereas the other half started with tactile cues being informative (bottom, squares) (see methods for details). (g) Mean response latency during the ASST according to genotype (two-way repeated-measures ANOVA, $P=0.6$) and group (one-way repeated-measures ANOVA, *Nos1^{+/+}*: $P=0.12$; *Nos1^{-/-}*: $P=0.35$). (h) Percentage of correctly completed trials according to genotype (two-way repeated-measures ANOVA, $P=0.15$) and group (one-way repeated-measures ANOVA, *Nos1^{+/+}*: $P=0.0002$; *Nos1^{-/-}*: $P=0.015$). (i) Number of trials performed for each block of the ASST according to genotype (two-way repeated-measures ANOVA, $P=0.5327$) and group (one-way repeated-measures ANOVA followed by post-hoc test including 5% false discovery rate, *Nos1^{+/+}*: $P=0.0028$; *Nos1^{-/-}*: $P=0.21$). (Number of trials done during the CDR block for *Nos1^{+/+}* vs. *Nos1^{-/-}* mice, paired t -test; $P=0.78$). (j) Percentage of perseverative errors during the CDR block (Mann-Whitney U test $p=0.0007$). (k) Comparison of normalized cumulative correct response rate as a function of the trial chronological order between the CD and CDR block. Dotted lines indicate linear regressions (slope: $P=0.055$ and $P=0.11$, elevation: $*P<10^{-7}$ and $P=0.39$ for *Nos1^{+/+}* and *Nos1^{-/-}* mice, respectively).

Values indicate means \pm SEM. $N>3$ independent litters. $*P<0.05$; $**P<0.01$; $***P<0.001$.

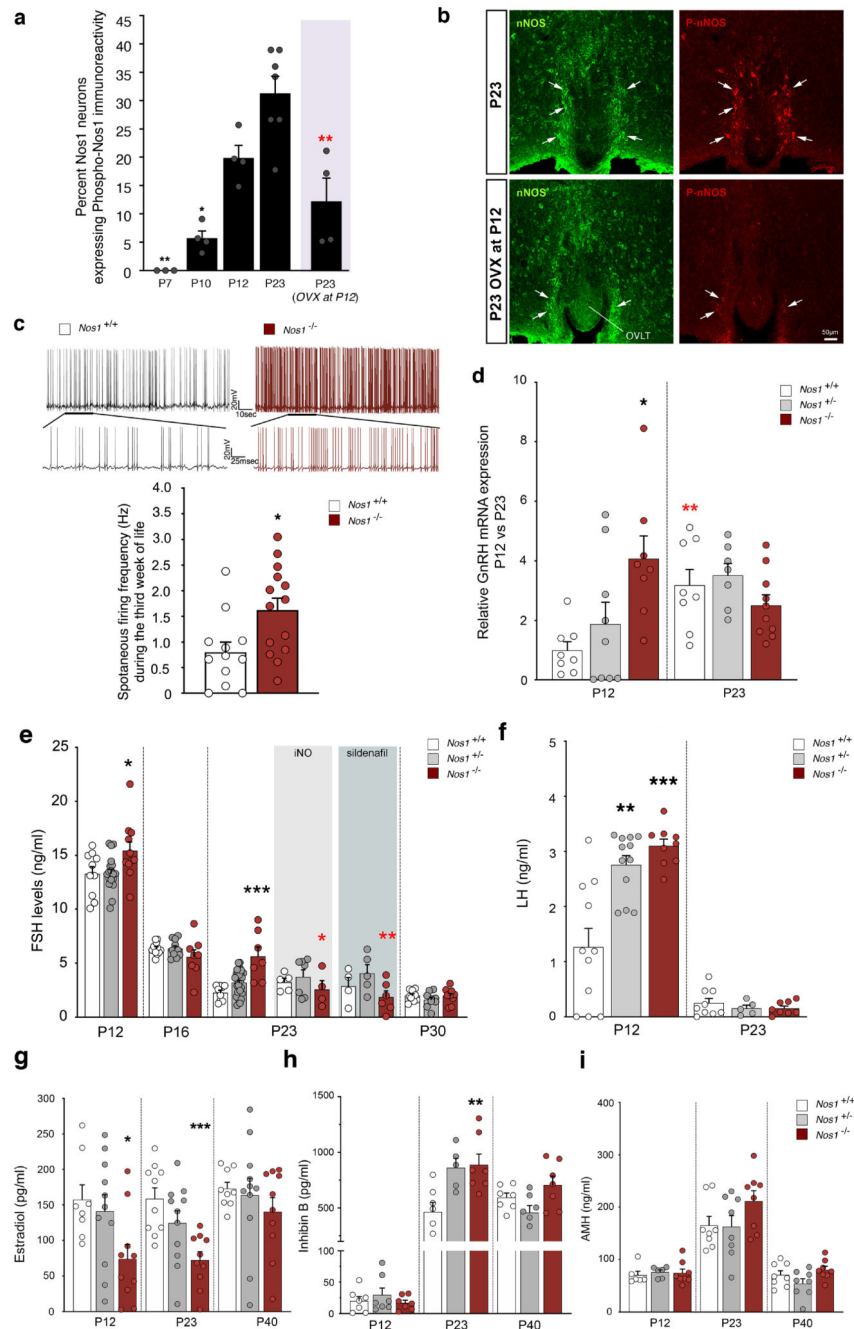


Figure 5. *Nos1* activity controls infantile GnRH neuronal function.

(a) Progressive phosphorylation of *Nos1* during postnatal development in the organum vasculosum laminae terminalis (OVLT) in intact female mice and females ovariectomized (OVX) on postnatal day 12 (P12). Bar graphs represent the mean ratio of *Nos1*-immunoreactive pixels to P-*Nos1*-immunoreactive pixels. P-*Nos1* levels are compared across developmental stages (one-way ANOVA with Tukey's post-hoc test, $n=3,4,4,7$). The values after ovariectomy at P12 are independently compared to P23 values (unpaired t-test, $n=7,4$).

- (b) Immunolabeling for Nos1 (green) and p-Nos1 (red) at P23 in the OVLT of intact (upper panel) of ovariectomized female mice (OVX at P12; bottom panel) showing migrating GnRH neurons (green) and Nos1 protein expression (red). N>3 independent litters.
- (c) Electrophysiological recordings of the spontaneous activity of preoptic area GnRH neurons in late infantile (P14-P21) *Gnrh::Gfp; Nos1^{+/+}* and *Gnrh::Gfp; Nos1^{-/-}* bigenic mice. Upper panels: representative trace of spontaneous firing in a GnRH neuron from a *Nos1^{+/+}* (left panel) and a *Nos1^{-/-}* (right panel) animal. The bottom trace shows an expansion of a small region of the top trace. Bottom panel: quantification of spontaneous firing frequency in GnRH neurons from *Gnrh::Gfp; Nos1^{+/+}* and *Gnrh::Gfp; Nos1^{-/-}* mice (unpaired t-test, n=12,14 cells, N=5,6 mice).
- (d) RT-PCR analysis of *Gnrh* expression in FACS-isolated GnRH-GFP neurons from *Gnrh::Gfp; Nos1^{+/+}*, *Gnrh::Gfp; Nos1^{+/-}* and *Gnrh::Gfp; Nos1^{-/-}* bigenic mice at P12 (n=8,9,8) and P23 (n=8,7,10). *Gnrh::Gfp; Nos1^{+/+}* values are compared to those of *Gnrh::Gfp; Nos1^{+/-}* and *Gnrh::Gfp; Nos1^{-/-}* mice (Kruskal-Wallis test with Dunn's post-hoc test at P12 and one-way ANOVA with Dunnett's post-hoc test at P23) * P < 0.05; ** P < 0.01. Red asterisks: comparison between mice of the same genotype at P12 and P23 (Mann Whitney U test).
- (e) FSH levels at P12, P16, P23 and P30 in *Nos1^{+/+}*, *Nos1^{+/-}* and *Nos1^{-/-}* female mice treated or not with iNO (grey-shaded area) or Sildenafil (blue-shaded area) during the infantile period. FSH values for *Nos1^{+/+}* are compared to those of *Nos1^{+/-}* and *Nos1^{-/-}* mice for each group of measurements (one-way ANOVA with Dunnett's post-hoc test; P12: n=10,19,11; P16: n=11,11,8; P23: untreated, n=9,29,7; Sildenafil-treated, n=4,5,6; iNO-treated, n=5,7,4; P30: n=10,9,10; Kruskal-Wallis test with Dunn's post-hoc test at P23). Red asterisks: comparison between mice of the same genotype but subjected to different treatments (one-way ANOVA with Dunnett's post-hoc test).
- (f) LH levels at P12 (n=11,9,9) and P23 (n=12,5,8) in *Nos1^{+/+}*, *Nos1^{+/-}* and *Nos1^{-/-}* female mice. *Nos1^{+/+}* LH values are compared to those of *Nos1^{+/-}* and *Nos1^{-/-}* mice for each age (P12: Kruskal-Wallis test with Dunn's post-hoc test; P23: one-way ANOVA with Dunnett's post-hoc test). *** P<0.001. Values indicate means ± SEM. N=4-8 independent litters.
- (g-i) Estradiol, (g) inhibin B (h) and AMH (i) levels at P12, P23 and P40 in *Nos1^{+/+}*, *Nos1^{+/-}* and *Nos1^{-/-}* female mice. P12: n=8,10,10 (g); n=7,7,7 (h); n=6,6,8 (i). P23: n=10,11,10 (g); n=7,5,7 (h); n=8,8,8 (i). P40: n=9,11,10 (g); n=7,7,7 (h); n=8,8,8 (i). *Nos1^{+/+}* LH values are compared to those of *Nos1^{+/-}* and *Nos1^{-/-}* mice for each group of measurements (g,h: one-way ANOVA with Dunnett's post-hoc test; i: Kruskal-Wallis test with Dunn's post-hoc test). Values indicate means ± SEM. N=3-8 independent litters. *P<0.05; **P<0.01; ***P<0.001.

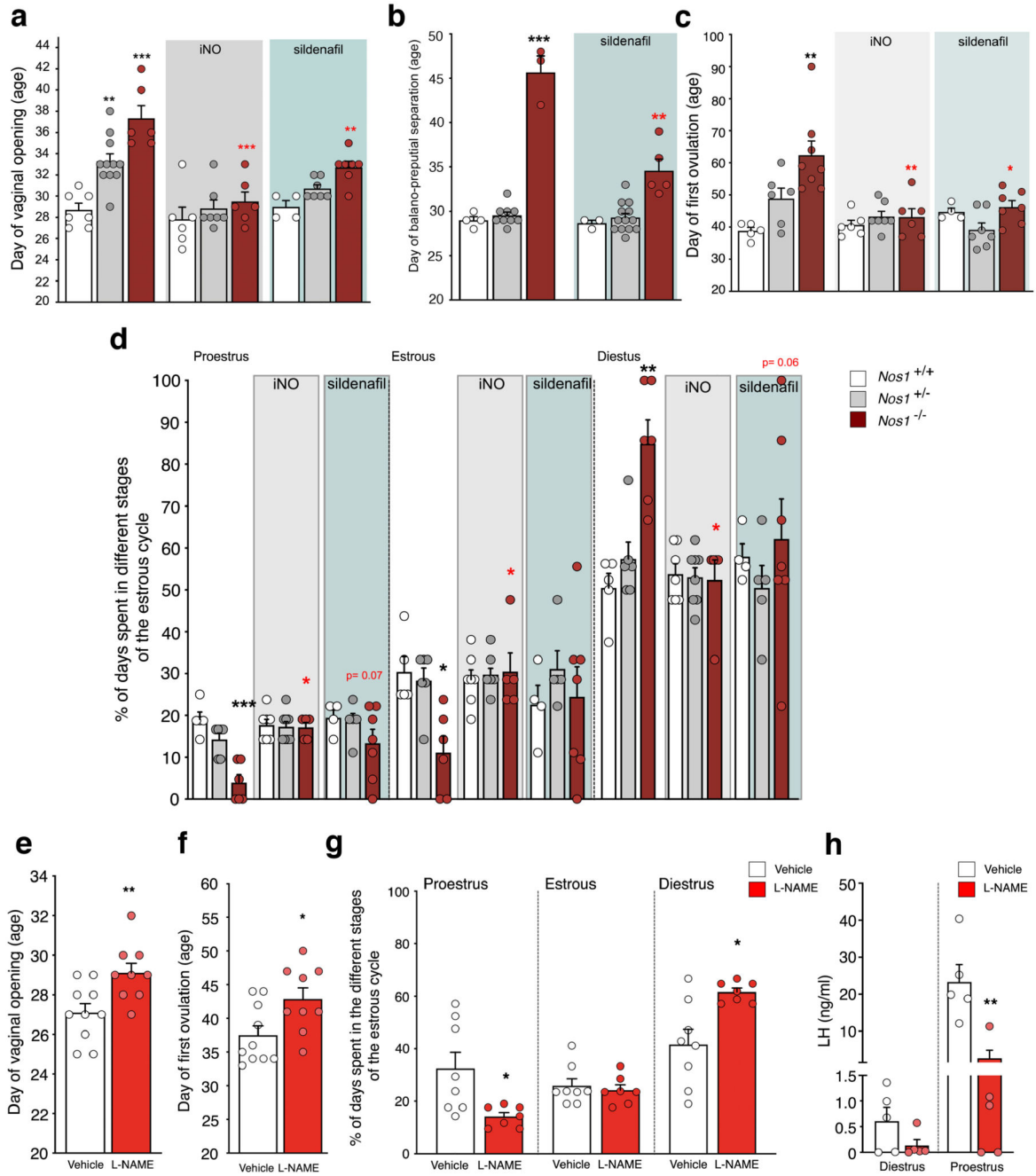


Figure 6. The action of NO during the critical infantile period is required for establishing a sexually mature phenotype.

(a) Age at vaginal opening or (c) puberty and (d) adult estrous cyclicity in *Nos1*^{+/+}, *Nos1*^{+/-} and *Nos1*^{-/-} female mice untreated (a: n=7,11,6; c: n=5,6,8; d: n=5,6,6) or treated with iNO (grey-shaded area, a: n=6,7,6; c: n=6,7,6; d: n=7,8,5) or Sildenafil (blue-shaded area, a: n=4,7,7; c: n=4,7,7; d: n=4,5,7) during the infantile period. *Nos1*^{+/+} values are compared to those of *Nos1*^{+/-} and *Nos1*^{-/-} mice for each group of measurements [one-way ANOVA with Dunnett’s post-hoc test for a (untreated) or Kruskal-Wallis with Dunn’s post-hoc test were used as detailed in Table S2]. Red asterisks: comparison between mice of the same

genotype but subjected to different treatments (a: one-way ANOVA with Dunnett's post-hoc test, b,d: Kruskal-Wallis with Dunn's post-hoc test). (b) Age at balanopreputial separation in *Nos1^{+/+}*, *Nos1^{+/-}* and *Nos1^{-/-}* male mice untreated (n=4,9,3) or treated with Sildenafil (blue-shaded area, n=3,13,5). *Nos1^{+/+}* values are compared to those of *Nos1^{+/-}* and *Nos1^{-/-}* mice for each group of measurements (Kruskal-Wallis test with Dunn's post-hoc test).

Red asterisks: comparison between mice of the same genotype but subjected to different treatments (unpaired t-test).

(e-h) Age at vaginal opening (e) and puberty (f) (unpaired t-test; n=10,9), and adult estrous cyclicity (g) (Mann-Whitney U test; n=8,7) after daily injections of vehicle or L-NAME during the infantile period.

(h) LH levels in diestrus and proestrus female mice subjected or not to LNAME treatment during the infantile period (Mann-Whitney U test; n=5,5). ** P = 0.008.

Values indicate means \pm SEM. N>3 independent litters. *P<0.05; **P<0.01; *** P<0.001.

Table 1
Genotype and clinical phenotype of six probands with ultra-rare heterozygous *NOS1* mutations

Subject	Sex	<i>NOS1</i> mutations	rs number	MAF %	Diagnosis	Inheritance	Associated Phenotyp
A	II-1	M	c.691G>A [p.Ala231Thr]	-	absent	nCHH	sporadic -
B	II-1	M	c.779G>A [p.Arg260Gln]	rs547371716	0.0019	KS	familial supernumerary tooth
C	II-1	M	c.3320C>T [p.Thr1107Met]	rs201943901	0.0064	KS	familial bilateral cryptorchidism micropenis crowded teeth
D	II-1	F	c.3370G>A [p.Glu1124Lys]	rs372660293	0.0055	KS	familial scoliosis osteoporosis
E	II-1	M	c.3370G>A [p.Glu1124Lys]	rs372660293	0.0055	nCHH	sporadic bilateral hearing loss obesity
F	II-1	F	c.3669A>G [p.Ile1223Met]	-	absent	nCHH	sporadic intellectual disability left hearing loss

Nucleotide and protein changes are based on reference cDNA sequence NM_000620.4. Nucleotide and protein changes are based on reference cDNA sequence NM_000620.4. Abbreviations are as follows: MAF, minor-allele frequency in gnomAD exome controls; CI congenital hypogonadotropic hypogonadism; nCHH, normosmic CHH; KS, CHH plus anosmia (Kallmann syndrome); M, male female. Bold: associated phenotypes present in *Nos1* deficient mice.